Are maps of nitrate reduction in groundwater altered by climate and land use changes?

Ida Karlsson Seidenfaden[1], Torben Obel Sonnenborg[1], Jens Christian Refsgaard[1], Christen Duus Børgesen[2], Jørgen Eivind Olesen[2], Dennis Trolle[3]

[1]Geological Survey of Denmark and Greenland, GEUS, Copenhagen, 1350, Denmark
[2]Aarhus University, Department of Agroecology, Tjele, 8830, Denmark
[3]Aarhus University, Department of Bioscience - Lake Ecology, Silkeborg, 8600, Denmark

Correspondence to: Ida K. Seidenfaden, ika@geus.dk

Abstract. Nitrate reduction maps have been used routinely in Northern Europe for calculating efficiency of remediation measures and impact of~~n~~ climate change on nitrate leaching. These maps ~~and~~ are ~~as such~~therefore valuable tools for policy analysis and mitigation targeting. Nitrate reduction maps are normally based on output from complex hydrological models, and once generated, are largely assumed constant in time. However, the distribution, magnitude and efficiency of nitrate reduction can not necessarily be considered stationary during changing climate and land use as flow paths, nitrate release timing and their interaction may shift. This study investigates the potential for ~~error~~erroneous nitrate impact projections~~s~~ when a constant nitrate reduction map is assumed during land use and climate change, both for nitrate ~~N~~ loads and the spatial variation in reduction. For this purpose, a crop and soil model (Daisy) was setup up to provide nitrate input to a distributed hydrological model (MIKE SHE) for an agricultural catchment in Funen, Denmark. Nitrate reduction maps based on an observed dataset of land use and climate were generated and compared to nitrate reduction maps generated for all combinations of four potential land use change scenarios and four future climate model projections. Nitrate reduction maps were found to be more sensitive to changes in climate, leading to reduction map change of up to 10%; while land use changes effects were minor. The study, however, also showed that the reductions maps are products of a range of complex interactions between water fluxes, nitrate use and timing. What is also important to note, is that the ~~and that the combination of the~~ choices made for ~~selected~~ future scenarios, model ~~formulations~~ setup and assumptions ~~are critical for~~may affect the resulting span in reduction capability. To account for this uncertainty multiple approaches, assumptions and models could be applied for the same area, however as these models are very time consuming this is not always a feasible approach in practice. An uncertainty in the order of 10% on the reduction map may have major impacts on practical water management. ~~(Hansen et al., 2017)~~ It is therefore important to acknowledge if such errors are deemed acceptable in relation to the purpose and context of specific water management situations.

formaterede: Engelsk (USA)

1 Introduction

Nitrate loads from agricultural areas are recognized to cause harmful impacts on groundwater and surface water resources, including eutrophication in aquatic ecosystems (Diaz and Rosenberg, 2008). This is also the case in the Baltic Sea drainage basin (Reusch et al., 2018), including Denmark, where nitrate load from agriculture constitutes one of the major water resources management challenges. When assessing the impacts of nitrate leaching from agricultural areas on aquatic ecosystems, the natural removal of nitrate in the groundwater and the surface water must be considered. This removal, often referred to as denitrification, retention or reduction, takes place via natural biogeochemical reduction processes. It can be expressed as a percentage removal and depending on the actual hydrobiogeochemical conditions the removal may mainly occur in groundwater or in surface water systems such as lakes or wetlands (Huno et al., 2018; Quick et al., 2019).

In the groundwater zone, nitrate reduction (nitrate ~~N~~ reduction) takes place when nitrate containing water migrates from aerobic to anaerobic conditions and inherent reduced compounds are available (Hansen et al., 2014a; Postma et al., 1991). For quaternary sediments these reduced compounds are mainly organic carbon and pyrite and ferrous ion from clay minerals (Ernstsen and Mørup, 1992; Postma et al., 1991). This transition zone between aerobic and anaerobic conditions is denoted the redox interface. The amount of nitrate reduction occurring in groundwater will then depend~~s~~ on the flow paths and the depth to the redox interface. In areas with Quaternary sediments characterized by groundwater dominated flow patterns and a relatively shallow redox interface, the nitrate ~~N~~ reduction in groundwater can be the dominant removal process (Hansen et al., 2009). For example, Højberg et al. (2015a) estimated that on average 63% of the nitrate leaching in Denmark is removed by nitrate ~~N~~ reduction in groundwater.

Heterogeneities in geology and drainage systems are responsible for substantial local spatial variations in nitrate ~~N~~ reduction. However, the spatial variation of nitrate reduction in the groundwater system has so far only been investigated in a handful of studies (e.g. Højberg et al., 2015a; Knoll et al., 2020; Kunkel et al., 2008; Merz et al., 2009; Tesoriero et al., 2015; Wriedt and Rode, 2006). Different approaches have been used in these studies from nitrate groundwater modelling (Højberg et al., 2015b; Merz et al., 2009; Wriedt and Rode, 2006), data driven machine learning (Knoll et al., 2020) or statistical modelling (Tesoriero

et al., 2015). A ~~newer~~n approach for utilizing and illustrating the results and the spatially varying nitrate removal fractions (percentages) are through a nitrate~~N~~ reduction map~~s~~ (Hansen et al., 2014a). A nitrate reduction map is~~Maps have~~ typically ~~been~~ produced by using a complex hydrological model~~s~~, including simulations of root zone nitrate leaching as well as groundwater and surface flow and transport; and have been applied in several catchments in Denmark and in catchments surrounding the Baltic Sea region (Hansen et al., 2014b; Højberg et al., 2017; Wulff et al., 2014). Hansen et al. (2014a) produced nitrate ~~N~~ reduction maps ~~with a 100 m spatial resolution~~ for a 101 km^2 catchment in Denmark, showing that nitrate ~~N~~ reduction may vary from 20% to 70% between neighbouring agricultural fields located only a couple of hundred meters apart. Similarly, Højberg et al. (2015a) and Andersen et al. (2016) estimated very large variations in nitrate ~~N~~ reduction between different regions in Denmark and in the Baltic Sea drainage basin, respectively. ~~When designing and targeting locations of mitigation measures, it is therefore important to consider how large a fraction of the nitrate leaching from the root zone in specific areas are removed during transport from the root zone to the point of discharge into the sea.~~

The efficiencies of remediation measures at different locations on nitrate loadings ~~on N loadings~~ can easily be calculated with a nitrate~~N~~ reduction map~~s~~, and the measures can be spatially targeted to locations, where the natural removal is relatively small and the mitigation effect hence is relatively large (Hansen et al., 2017; Refsgaard et al., 2019). Similarly, a nitrate ~~N~~ reduction map~~s~~ can be used to transform climate change and other land use changes impacts on nitrate leaching from agricultural areas to a catchment response (Olesen et al., 2019). Using nitrate ~~N~~ reduction maps based on a single model run, ~~is~~ clearly a much faster method than running multiple complex hydrological simulation models for large ensembles of ~~, and~~scenarios and is therefore a practical tool for policy analysis (Andersen et al., 2016; Højberg et al., 2015a). A severe problem in this respect is, however, that the ~~N~~ nitrate reduction maps may ~~are~~ not be constant in time as the reduction taking place at a given location ~~but~~ depend on ~~the amount of rainfall and~~ resulting flow pathways (Hansen et al., 2014b). It is therefore ~~A~~very relevant ~~question~~to investigate ~~is therefore how large errors are made~~the potential error arising~~,~~ when nitrate ~~N~~ reduction maps are assumed to be constant in time. No studies have been reported on that issue. Even as, the link between climate change, land use change and nitrate reduction has been established in ~~multiple~~previous studies (e.g. Fleck et al., 2017; Mas-Pla and Menció, 2019; Olesen et al., 2019; Ortmeyer et al., 2021; Sjøeng et al., 2009), Ortmeyer et al. (2021) used a water balance model

Feltkode ændret

combined with a lumped-parameter nitrate mass model for an area in Germany, finding that nitrate concentrations in the groundwater increased towards the end of the century by up to 89 % as a result of changes in temperature, evapotranspiration and precipitation. Mas-Pla and Menció (2019) found that climate change in turn affects groundwater recharge and thus the dilution of nitrate in the subsurface in a study in Catalonia. While, Paradis et al. (2016) found that new agricultural practices under changing climate conditions led to substantial nitrate increases on an Island in eastern Canada. ~~; finding that as land use changes affect input, distribution and timing of nutrients; climate change in turn affects groundwater recharge, water balance and subsurface flow paths (Mas-Pla and Menció, 2019; Olesen et al., 2019; Ortmeyer et al., 2021).~~

The objectives of the present study are to assess i) how ~~N~~nitrate ~~-~~reduction maps showing spatially varying nitrate removal fractions in the groundwater zone are affected by changes in climate and land use, and ii) the errors in ~~N~~ nitrate loading made by assuming ~~N~~nitrate ~~-~~reduction maps to be constant. The analyses are performed using a complex hydrological simulation model for a Danish catchment to calculate nitrate ~~N~~ ~~-~~reduction maps for the present conditions as well as for scenarios of climate and land use change. The reduction in this catchment has previously been shown to be dominated by saturated zone reduction processes (Hansen et al., 2009).

2 Study site

The study site is located in the central part of Denmark on the Island of Funen. It consists of the 486 km^2 upstream part of the Odense River basin, where the Kratholm discharge station marks the outlet (Figure 1~~Figure 1~~). The catchment is drained by a 200 km river network with the outlet located at the Odense Fjord to the northeast. Land use in the area is predominantly agricultural (68%), mainly pig farms followed by dairy and plant production farms (Figure 1~~Figure 1~~); forest constitute only 5 %; urban areas are 8%; 1% is water bodies and the remaining are either fellow or grasslands (Nielsen et al., 2000). The soil map and parameters consists of 10 soil types that are created by Børgesen et al. (2013) and Greve et al. (2007) based on national databases Børgesen et al. (2013); Greve et al. (2007). The soil type is dominated by clayey soils (71%) with smaller areas of sand (see Karlsson et al. (2015) and Karlsson et al. (2016) for more information). as a results the agricultural area is heavily drained. The geology is mainly a result of previous glaciations like till deposits. Aquifers are generally confined and the

formaterede: Engelsk (USA)

Feltkode ændret

formaterede: Dansk
formaterede: Dansk
Feltkode ændret
Feltkode ændret
formaterede: Dansk
formaterede: Dansk
Feltkode ændret
formaterede: Dansk

phreatic groundwater tables are shallow. The discharge station at Kratholm (ST45.21) has one of the best nutrient time series in Denmark starting in the 1980s, with near-daily sampling from 1989 (Windolf et al., 2016). The station~~,~~, therefore, provid~~es~~ing a long and near-complete data set for nutrient modelling as well as an extensive water discharge time series (Trolle et al., 2019). In 2005-2009, t~~T~~he average discharge amounts to 4.4~~6~~m^3/s and the load is approximately 14 kg NO_3-N/ha/year. A decreasing trend in nitrate loads has been observed previously during 2000-2013 by Windolf et al. (2016), possibly due to implementation of mitigation measures in the catchment. ~~The geology is mainly a result of previous glaciations like till deposits. Aquifers are generally confined and the phreatic groundwater tables are shallow.~~ Three other discharge stations are also present in the catchment (from downstream: ST45.01, ST45.28, ST45.20)

~~There were~~ 226 measurements of the redox depth are available from boreholes in the area, the redox depths were mainly interpretated based on sediment colour as described by e.g. Ernstsen and Mørup (1992), and a few by measurements of reduced compounds. They show a ~~fairly~~ shallow redox interface, where 50% of the measurements have a redox depth less than 4.5 m below terrain, while 90 % of the depths are located in the upper 12.9 meter. An old redox depth map with 1 km resolution, based on measurements and geological interpretation, shows depths between 1 to 5 meters at many locations and between 5 to 15 meters in other locations (Ernstsen et al., 2006). A recent redox depth map of Denmark was created in 2019, where measurements and system variables were used in a machine learning environment to create a detailed ~~100 meter~~ redox depth map in 100 meter resolution~~(Koch et al., 2019b)~~. This newer map also indicates that the redox depth in the study area is predominantly shallow with 1-10 meter depth, and very few sites of 10-15 meters depth (Koch et al., 2019a; Koch et al., 2019b).

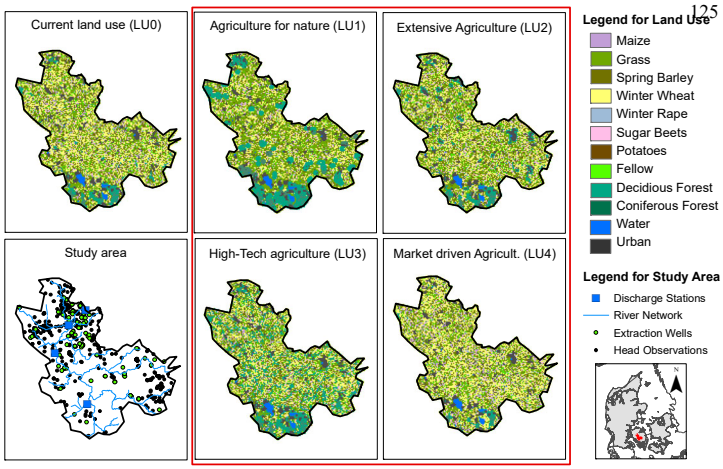

Figure 1: The current land use distribution (LU0) in the study area (Upper left panel) and the river network and location of observations and extraction wells (Lower left panel). The ~~R~~red square ~~shows the current land use, the river network and water extraction wells and head observations in the catchment: The current land use distribution (LU0) in the study area (Upper left panel) and the river network and location of observations and extraction wells (Lower left panel). The remaining panels~~ **(right and center)** marks the~~shows~~ four **projected scenarios for land use scenarios LU1-4.**

3 Methods

~~3.1 Daisy/MIKE SHE setup and calibration~~

The Daisy-MIKE SHE modeling system is used to describe nitrate transport in the catchment. Daisy is used to quantify leaching of nitrate from the root zone while MIKE SHE is used to simulate the transport and degradation of nitrate in the saturated zone. Both models are forced by the same daily inputs of precipitation, temperature and potential evapotranspiration. Both Mike She and Daisy have been used extensively in the danish area, and Mike She forms the basis of the national nitrate and groundwater model (Bruun et al., 2003; Hoang et al., 2010; Højberg et al., 2015a; Højberg et al., 2010; Højberg et al.,

2013; Højberg et al., 2015b; Troldborg et al., 2010). Mike She is a fully coupled integrated groundwater-surface water model and this integration is important for assessing the feedback between unsaturated and saturated zone, especially under changing climate. However, Mike She does not simulate crops development and nitrate leaching from the root zone, and therefore information from an agrological model, like Daisy, is necessary.

Calibration is done in ~~three~~three phases ~~steps~~: 1. The MIKE SHE model is inverse automatically calibrated using discharge and hydraulic heads (section 3.1), for the calibrated model the spatial distribution of the redox interface is then assessed (section 3.1.1); 2. Daisy adopts calibrated soil parameter from MIKE SHE, ~~other~~additional flow and crop parameters are manually calibrated to catchment scale water balance and crop yield (section 3.2); 3.- The combined Daisy-MIKE SHE nitrate model is manually calibrated using the nitrate arrival percentage (section 3.3~~3~~) by adjusting the ~~location~~depth of the redox interface layer. ~~(section 3.4).~~ The modelling results are then used to create the nitrate reduction maps (section 3.4~~5~~) for a range of land use and climate scenarios (section 3.5~~6~~).

3.1 MIKE SHE setup and calibration (Phase 1)

MIKE SHE is a fully distributed hydrological model that is built as a modular system with configurable complexity of the different flow compartments (Abbott et al., 1986; Graham and Butts, 2005). To obtain consistency with the flow calculations in Daisy, the present MIKE SHE is also based on a 1D finite difference description of the unsaturated zone using Richards' equation, parameterized by van Genuchten (1980) formulations of the retention curve and the unsaturated hydraulic conductivity curve. A 3D finite difference description of the saturated zone based on Darcy's equation was selected, including a linear reservoir formulation of tile drainage flow. The study is heavily tile drained, and it can be assumed that drainage will always be present when it is need in the agricultural areas. ~~h~~However, the actual site-specific location of tile drains are unknown and therefore ~~D~~drains are specified across the entire catchment at a depth of -0.5 meters ~~Troldborg et al. (2010)following the approach of Troldborg et al. (2010) as the actual location of tile drains are unknown~~. Drain flow is however only activated when groundwater level rise above drain level. Apart from representing tile drainage the drainage system also represents small ditches and stream, too small to incorporate into the river system following the approach of Troldborg et al. (2010). River flow

is described using the MIKE 11 module, where a relatively simple routing method (Muskingum) is used. Additionally, physical formulations for evapotranspiration (Kristensen and Jensen, 1975) and 2D overland flow (DHI, 2019) are selected. The MIKE SHE model was calibrated using the build-in autocalibration scheme AutoCal (Madsen, 2000), which uses the global search function Population Simplex Evolution method. Calibration was carried out against data from four discharge stations and 455 groundwater wells with hydraulic head measurements from the period 2004-2007 and validated in the periods 2000-2003/2008-2009. The multi-objective function consists of water balance error (mean daily error) for the four discharge stations and RMSE for the hydraulic head measurements and three of the discharge stations (one discharge station, ST45.28, is omitted here due to human regulation on the flow system). After a sensitive analysis on 28 free parameters with 43 tied parameters; a total of five parameters were chosen for calibration, of these, one soil parameter in the unsaturated zone, one drainage parameter and three saturated zone parameters. A thorough description of the calibration scheme can be found in Karlsson et al. (2016).

3.1.1 Estimation of the redox interface

The redox interface for each cell in MIKE SHE is determined using a five step method developed by Hansen et al. (2014a). The method is based on the assumption that the present location of the redox interface is a result of the cumulative oxygen percolation through the soil column since the last ice age in the Holocene 11,700 BP.

The redox interface is assumed to have been at ground level at the end of the glaciation and to have migrated downwards by an unknown number of millimeters per yearly recharge. Following the procedure of Hansen et al. (2014a), first step is therefore to find the average yearly recharge, by running a model simulation without anthropogenic influences (abstraction and tile drainage). In the second step, the different redox capacities in soils are accounted for, where the capacity of sandy soils are multiplied with a factor of three compared to value specified for the clayey soil types applying the classification from Børgesen et al. (2013) and Greve et al. (2007). The third step generates the redox interface expressed through equation (3):

$$Redoxdepth_i = flux_i * f + min.redoxdepth$$

where $Redoxdepth_i$ is the redox depth (m) calculated at each grid (i), $flux_i$ is the groundwater recharge (m/yr) which is multiplied by the migration constant f (yr) (Hansen et al., 2014a). The upper part of the unsaturated zone is assumed to have no redox capacity due to very fast air diffusion, which is accounted for using a minimum redox depth, min.redoxdepth (m). To account for unrealistically high values of the redox depth, a maximum redox depth is also estimated based on the principles of Hansen et al. (2014). Hereby, the spatially distributed redox interface layer is quantified and incorporated into MIKE SHE (step four). The final step (five) is the calibration of the depth of the redox interface layer also described as the calibration of the nitrate model by adjusting the location of the layer. Step five will be described in section 3.3.

3.2~~2~~ Daisy setup and calibration (Phase 2)

Daisy provides a one-dimensional finite difference description of soil-water-crop-atmosphere processes (Abrahamsen and Hansen, 2000; Hansen et al., 1991) where flow is described using Richards' equation and to a minor extent by macro pore flow for loamy soils (Hansen et al., 2012a). Nitrate transport is driven by the convection-dispersion algorithm in the soil matrix. The one-dimensional Daisy model can be used to represent an entire catchment by combining multiple columns of Daisy computations and evaluating the summed water balance. Calibration on catchment scale is however not straightforward and must be done manually and in an incremental manner, due to the large number of 1D model columns.

The Daisy model setup for the Odense is contains on ~~R~~roughly 12,000 1D Daisy columns, and the water balance module is based on a previous calibration of the catchment (Børgesen et al., 2013), where root zone leaching and groundwater abstraction is compared with river discharge (Børgesen et al., 2013; Refsgaard et al., 2011). The model is setup so that each column ~~are setup up in this study to repr~~ represent unique combinations of soil type, climate, crop rotation and groundwater depth~~.~~. The Daisy model uses the same climate input and soil parameter setup as MIKE SHE and the sensitive and calibrated unsaturated soil parameter~~s~~ from MIKE SHE were therefore transferred to Daisy ~~from MIKE SHE~~. A more detailed description of the

Daisy setup can be found in Karlsson et al. (2016). The water balance performance of Daisy was evaluated in the same calibration (2004-2007) and validation periods (2000-2003/2008-2009) as MIKE SHE ~~(2004-2007/2000-2003/2008-2009)~~. ~~The one-dimensional Daisy model uses the same climate input as MIKE SHE and calibrated soil parameters were transferred from MIKE SHE. Tidligere cali (borgsen 2013), vand balance er tjekket refsgaard 2011 GEUS vandbalance i DK~~

~~Further calibration of the flow compartment of Daisy against observed stream flow sums at the catchment outlet was done manually by comparing to accumulated perlocation from all 12,000 columns, following methods proposed by Allen et al. (1998) and Styczen et al. (2004). Thus, water balance consistency was ensured by calibrating Daisy and MIKE SHE such that they produce similar actual evapotranspiration and stream flow for the simulation period.~~

Daisy also simulates nitrate leaching for each soil column that represents a unique combination of soil type, climate, crop rotation and groundwater depth. Crops are fertilized with mineral and organic nitrogen dependent on the farm type and soiltype~~only and at t~~. The crop recommended ~~N~~ nitrogen~~N~~ rate for the years ~~(~~2004-2007~~)~~ was used to setup the fertilization scheme. Nitrate leaching ~~-~~input are ~~estimated~~simulated on ~~as~~ daily basis ~~average n~~based on the ~~itrate N leaching of the~~ leaching from the permutated crop rotations simulated for the dominating soil type within a 200m x 200 m square grid (Karlsson et al., 2016). Because of the close feedback mechanism between nitrogen~~N~~ yields and ~~N-~~ ~~-~~nitrate leaching, the simulated mean nitrogen~~N~~ yields were recalibrated to observed annual mean nitrogen yields on Funen (Statistikbanken, 2015) for the dominating soil type for the period 2004-2007. The calibration is conducted ~~-~~by adjusting the crop parameters~~. Again~~, following the methodology of ~~Allen et al. (1998) nd~~ Styczen et al. (2004). Nitrogen concentrations of yields were extracted from table values of~~s on~~ mean nitrogen~~N~~ contents for different crops (Møller et al., 2005). For crop rotations including clover grass and peas nitrogen biological fixation is calculated using Høgh-Jensen et al. (2004) and nitrogen atmospheric deposition is included as input to the soil using standard Daisy settings for dry and wet deposition ~~Hansen et al. 2012~~ (Hansen et al., 2012b).

In the simulations under climate change, the effect of change CO_2 concentration in the atmosphere has an impact on the light saturated photosynthesis rate (Fm parameter), which is a crop parameter~~not included~~ in the Daisy crop model code. In order

formaterede: Engelsk (USA)
formaterede: Engelsk (USA)
formaterede: Ikke Fremhævning
formaterede: Ikke Fremhævning
formaterede: Ikke Fremhævning
formaterede: Engelsk (USA)
formaterede: Fremhævning

to deal with this feedback mechanism, the procedure to change the Fm parameter was adopted from ~~described in~~ Børgesen and Olesen (2011) ~~was adopted~~.

~~MIKE SHE is a fully distributed hydrological model that is built as a modular system with configurable complexity of the different flow compartments (Abbott et al., 1986; Graham and Butts, 2005). To obtain consistency with the flow calculations in Daisy, the present MIKE SHE is also based on a 1D finite difference description of the unsaturated zone using Richards' equation, parameterized by van Genuchten (1980) formulations of the retention curve and the unsaturated hydraulic conductivity curve. A 3D finite difference description of the saturated zone based on Darcy's equation was selected, including a linear reservoir formulation of tile drainage flow. Drains are specified across the entire catchment as the actual location of tile drains are unknown. Drain flow is however only activated when groundwater level rise above drain level. River flow is described using the MIKE 11 module, where a relatively simple routing method (Muskingum) is used. Additionally, physical formulations for evapotranspiration (Kristensen and Jensen, 1975) and 2D overland flow (DHI, 2019) are selected. The MIKE SHE model was calibrated using the build-in autocalibration scheme AutoCal (Madsen, 2000). Calibration was carried out against data from four discharge stations and 455 groundwater wells from the period 2004-2007, see Karlsson et al. (2016) for details.~~

~~The one-dimensional Daisy model uses the same climate input as MIKE SHE and calibrated soil parameters were transferred from MIKE SHE. Further calibration of the flow compartment of Daisy against observed stream flow sums at the catchment outlet was done manually by comparing to accumulated perlocation from all 12,000 columns, following methods proposed by Allen et al. (1998) and Styczen et al. (2004). Thus, water balance consistency was ensured by calibrating Daisy and MIKE SHE such that they produce similar actual evapotranspiration and stream flow for the simulation period.~~

~~3.2 Nitrate simulations in Daisy~~

~~Daisy simulates nitrate leaching for each soil column that represents a unique combination of soil type, climate, crop rotation and groundwater depth. Crops are fertilized with mineral nitrogen only and at the crop recommended N rate (2004-2007). N-input are estimated as daily average nitrate N leaching of the permutated crop rotations simulated for the dominating soil type~~

~~within a 200m x 200 m square grid (Karlsson et al., 2016). Because of the close feedback mechanism between N yields and N leaching, the simulated mean N yields were recalibrated to observed annual mean yields on Funen (Statistikbanken, 2015) for the dominating soil type for the period 2004-2007 by adjusting the crop parameters. Again following the methodology of Allen et al. (1998) and Styczen et al. (2004). N concentrations of yields were extracted from tables on mean N contents for different crops (Møller et al., 2005).~~

~~In the simulations under climate change, the effect of change CO_2 concentration in the atmosphere has an impact on the light saturated photosynthesis rate (Fm parameter), which is not included in the Daisy crop model code. In order to deal with this mechanism, the procedure described in Børgesen and Olesen (2011) was adopted.~~

3.~~33~~ ~~The Nitrate model: Daisy/MIKE SHE~~Calibration of the nitrate model (Phase 3)

The nitrate model is then constructed by combining the two models, Daisy and MIKE SHE. Daily values of nitrate flux from Daisy serves as input to MIKE SHE, where nitrate transport is simulated by converting ~~-~~nitrate input to particles using the particle-tracking module. Each time the accumulated input of nitrate reach 0.5 kg N within the model cell (200mx200m), a particle is released from the water table and is allowed to follow the groundwater flow. If the particle penetrates the redox interface, the nitrate is assumed to be removed completely and instantaneously by denitrification (Hansen et al., 2014a; Postma et al., 1991). Remaining particles will emerge in discharge zones typically located in stream valleys and leave the catchment at the river outlet (Kratholm station). The nitrate arrival percentage (NAP) is found as the accumulated amount of ~~N~~ nitrate leaving the catchment divided by the amount released at the water table.

The nitrate model is then calibrated by adjusting the depth to the redox interface through the calibration of f and min.redoxdepth to obtain the observed NAP (step five)~~was calibrated by adjusting the depth to the redox interface (see section 03.4) until an acceptable match to the observed NAP was obtained~~. ~~A more detailed analysis and description of the nitrate transport method can be found in Hansen et al. (2014b).~~

~~3.4 Estimation of depth to redox interface~~

Formateret: Normal, Mellemrum Før: 0 pkt., Efter: 0 pkt., Hold ikke linjer sammen

~~The redox interface depth for each cell in MIKE SHE is determined using a five step method developed by Hansen et al. (2014a). The method is based on the assumption that the present location of the redox interface is a result of the cumulative oxygen percolation through the soil column since the last ice age in the Holocene 11,700 BP.~~

~~The redox interface is assumed to have been at ground level at the end of the glaciation and to have migrated downwards by an unknown number of millimeters per yearly recharge. Following the procedure of Hansen et al. (2014a), first step is therefore to find the average yearly recharge, by running a model simulation without anthropogenic influences (abstraction and tile drainage). In the second step, the different redox capacities in soils are accounted for, where the capacity of sandy soils are multiplied with a factor of three compared to value specified for the clayey soil types applying the classification from Børgesen et al. (2013) and Greve et al. (2007). The third step generates the redox interface expressed through equation (3):~~

~~$$Redoxdepth_i = flux_i * f + min.redoxdepth$$~~

~~where Redoxdepth$_i$ is the redox depth (m) calculated at each grid (i), flux$_i$ is the groundwater recharge (m/yr) which is multiplied by the migration constant f (yr) (Hansen et al., 2014a). The upper part of the unsaturated zone is assumed to have no redox capacity due to very fast air diffusion, which is accounted for using a minimum redox depth, min.redoxdepth (m). To account for unrealistically high values of the redox depth, a maximum redox depth is also estimated based on the principles of Hansen et al. (2014).~~

~~Hereby, the spatially distributed redox interface is quantified and incorporated into the MIKE SHE nitrate model (step four) and the location of the redox depth is then calibrated by adjusting f and min.redoxdepth to obtain the observed NAP (step five).~~ As the calibration of these two parameters may result in non-uniqueness, ~~,~~ all possible combinations (realisations) of the two parameters resulting in observed NAP, are identified. For all realisations the cumulative distribution of the redox depth is found at the location, where observations of redox depth are available from boreholes, as well as the cumulative distribution of the entire catchment. These two graphs are subsequently compared with the cumulative distribution of the actual measured redox depth in boreholes. The realization with the best representation of the fractional distribution of the observed redox depth for both on-site and especially catchment scale is chosen for the final redox depth parameters.

Formateret: Indrykning: Første linje: 0 cm

The reason for comparing calculated redox depths to cumulative distributions for actual measurement locations and the entire catchment distribution is due to several issues. First, measured redox depths are very local point measurements, and large variations in space (within a few meters) are often reported (e.g. Ernstsen, 1996; Hansen et al., 2008), and a measurement may not be representable for the area or model scale, where numerous measurements together are more likely to represent to the correct fractional distributions in the catchment. Furthermore, the calculated redox depth may be applicable on catchment scale, on which scale it is also calibrated, but less trustworthy on location scale. A more detailed analysis and description of the nitrate transport method can be found in Hansen et al. (2014b). ~~and subsequently compared with the measured redox depth in boreholes.~~

3.~~4~~5 Estimation of reduction map and map correction

The reduction map quantifies the nitrate reduction potential for each model grid (Hansen et al., 2014a). The number of representative particles released at each cell that is subsequently reduced is divided by the total number of particles released. The reduction map is therefore based on results from the nitrate model that is run with the calibrated redox interface. In the reduction map, a grid cell with the value of 100% indicates that all particles released in the cell are subsequently reduced, while a value of 50% indicates that half of all particles (nitrate) reaches surface waters unreduced. Therefore, it provides valuable information on what the environmental impact in terms of nitrate loading of farming practices are for specific parts of the landscape.

Unfortunately, during the release of particles in the MIKE SHE model, numerical issues occasionally cause some particles to get stuck in the unsaturated zone. Mike She is a commercial modelling tool and therefore there is no possibility to access the modelling code in order to correct this numerical error, or in any other way account for this model limitation. Therefore, it was necessary to introduced a correction scheme. The actual fate of these stuck particles (reduced/non-reduced) are ~~therefore~~ unknown. At an early stage the assumption was made that the captured particles, if they had moved correctly through the system, would be subject to a fate similar to the non-captured particles, i.e. that the relationship between reduced/non-reduced

was the same. If this assumption is valid the calculation the reduction potential in each grid cell is the same with/without the stuck particles. Unfortunately, this assumption may not always be valid. Furthermore, the arrival percentage estimated by the two methods are not the same as not all particles are released in the complex particle arrival count, the data from which is the only way to calibrate the nitrate model. For the two methods to be comparable it is therefore necessary to exclude the particles that are stuck in the unsaturated zone.~~If this assumption is valid the calculation of a direct arrival percentage (meaning a reduction map multiplied with the nitrate input) should give the same arrival percentage as calculated based on the more complex particle arrival count excluding these captured particles. However, this was unfortunately found not always to be the case.~~

~~As it was not possible to correct this numerical error in the model code, or in any other way account for this model limitation, a correction scheme was introduced.~~ The correction factor is therefore introduced to eliminate the particles that are stuck from changing the reduction map. The correction uses a simple linear equation, where ~~the~~ a correction factor is manually fitted so that the ~~direct~~ arrival percentage (originating from the reduction map multiplied by the nitrate input) matches the particle arrival percentage. These corrections are done individually for all reduction maps, and the correction causes a change in the reduction in the range of -7% to 9% with a mean of 2%.

3.~~5~~6 Climate and land use scenarios

The hydrological model was forced by 16 scenarios for future climate and land use. One emission scenario, the IPCC AR4 SRES A1B scenario (Nakicenovic et al., 2000) where chosen as the basis for this study. Since the study was conducted newer generations of emission scenarios have been developed by the IPCC (van Vuuren et al., 2011), known as the Representative Concentration Pathways (RCPs); the A1B scenario is generally comparable to the RCP6.0-emission scenario (medium scenario).

In this study, realizations from four climate model combinations, GCM-RCM couplings, were selected from the ENSEMBLES project (Hewitt and Griggs, 2004), where results from the period 2080-2099 were extracted and used as input to the

hydrological model. The reference evapotranspiration is calculated using FAO Penman– Monteith formula based on the climate model outputs for temperature, radiation, water vapour wind speed and water pressure. Precipitation d~~D~~ata from both this period and the reference period, 1990-2009, were bias-corrected (downscaled) using the DBS method, which is a direct method that preserves the dynamics and non-stationary nature of the raw climate model results (Seaby et al., 2013). While reference evapotranspiration was downscaled using a bias removal method (Seaby et al., 2013). The four selected realizations represent a wet, +19% in precipitation (ECHAM-HIRHAM5), a dry, -11% decrease in precipitation (ARPEGE—RM5.1), a warm, +3.4 °C temperature increase (HadCM3-HadRM3) and a model representing a median projection~~model~~, +10% in precipitation and +2.1 °C in temperature (ECHAM5-RCA3). The change factors can be seen in Table 1~~Table 1~~. Both climate models and bias-corrections are described in more detail in Karlsson et al. (2016).

Season mean	Climate model	CHANGE FACTOR		
		Precipitation	Temperature	RefET
Annual	ARPEGE–RM5.1	0.88	2.14	1.12
	ECHAM5–HIRHAM5	1.28	2.08	0.94
	ECHAM5–RCA3	1.17	2.22	0.94
	HadCM3–HadRM3	1.00	3.72	1.19
Fall	ARPEGE–RM5.2	0.74	2.05	1.23
	ECHAM5–HIRHAM6	1.20	2.45	1.02
	ECHAM5–RCA4	1.18	2.35	0.98
	HadCM3–HadRM4	0.93	4.11	1.33
Winter	ARPEGE–RM5.3	1.18	2.40	1.24
	ECHAM5–HIRHAM7	1.30	2.65	1.22
	ECHAM5–RCA5	1.30	2.64	1.03
	HadCM3–HadRM5	1.31	4.19	1.57
Spring	ARPEGE–RM5.4	0.95	1.83	1.03
	ECHAM5–HIRHAM8	1.33	1.72	0.92
	ECHAM5–RCA6	1.18	2.03	0.88
	HadCM3–HadRM6	1.02	3.24	1.07
Summer	ARPEGE–RM5.5	0.67	2.29	1.14
	ECHAM5–HIRHAM9	1.32	1.50	0.90
	ECHAM5–RCA7	1.02	1.88	0.96
	HadCM3–HadRM7	0.78	3.36	1.19

Table 1: Change factor for the four climate model combinations for precipitation (multiplicative), temperature (°C - additive) and reference evapotranspiration (multiplicative)

The four climate model realizations were combined with four land use scenarios. The land use scenarios were created during workshops with researcher, farming industries, environmental protection agencies and government representatives. During the workshops, participants identified possible paths of developments for the land use in Denmark considering the balance of agricultural marked value on one side and priorities in the society on the other (e.g., environmental concerns or recreational use). From the workshop four scenarios that describe agricultural management in the period 2080-2099 was created, as: LU1: "Agriculture for nature", where the agricultural area is reduced to 40% of the land area through afforestation and increasing grass areas and fertilization rates are generally reduced (-40%); LU2: "Extensive agriculture" with a small 3% ~~point~~ p.p. reduction in agricultural area resulting in 64% farmland; however, some of the intensive farm types (with high fertilization rates) are converted to less intensive farm types with less fertilization (total change of -60%); LU3: "Hightech agriculture", also with a small decrease in agricultural area of 3%, but with a productivity of crops that is assumed to increase, resulting in an insignificant change in the needed fertilizer inputs (0%); LU4: "Market driven agriculture", where forest and some extensive farm types are converted into intensive farming resulting in an agricultural area of 70%. At the same time, fertilization rates are increased to reach maximum production (+20%). More information on the land use scenarios can be found in Olesen et al. (2014) and Karlsson et al. (2016).

All ~~16~~ 20 combinations of future climate projections (4) and land use (5) were specified as input to the hydrological model. The model was run for both future (2088-2099) and ~~and compared to the climate model results found for the~~ reference period (1990-2009) ~~using the same land use scenarios,~~ resulting in ~~32~~ 40 scenarios. Additionally, the model was run with observed climate for the period 1990-2009 (5 scenarios using observed land use and the four land use scenarios) ~~and observed land use for the period 1990-2009 (combined with the observed climate and results from the four climate models)~~. Hence, a total of 4550 ~~50~~ model simulations were analyzed (Table 2~~Table Table 3~~). In this paper the following terminology is used:

- Observational period: Results from a hydrological model and the rootzone model Daisy run forced with observational data in the period 1990-2009. This period covers both the calibration period (2004-2007) and validation periods (2000–2003 and 2008–2009), all of which are driven by observational data.
- Reference period: This period is used to describe specifically the climate model driven hydrological results from the period 1990-2009. Future climate model runs are always compared with results from this period for the relevant climate model to ensure that climate model biases do not dominate the results.
- Future period: The future scenario refers to climate model forced runs for the period 2088-2099.
- Baseline: The term baseline refers to results from the specific model run combination (scenario number~~no.~~ 1, Table 3), where current land use scenario (LU0) is combined with the observational climate data.

		Land use (LU) scenario				
Period	Climate	Baseline	Agriculture for nature	Extensive agriculture	High-tech agriculture	Market driven agriculture
Control period, 1990-2009	Obs. Climate	1	2	3	4	5
	ECHAM5–HIRHAM5	6	7	8	9	10
	ECHAM5–RCA3	11	12	13	14	15
	ARPEGE–RM5.1	16	17	18	19	20
	HadCM3–HadRM3	21	22	23	24	25
Future period, 2080-2099	ECHAM5–HIRHAM5	26	27	28	29	30
	ECHAM5–RCA3	31	32	33	34	35
	ARPEGE–RM5.1	36	37	38	39	40
	HadCM3–HadRM3	41	42	43	44	45

Table 2~~3~~: Land use and climate scenario matrix showing the scenario numbers. Shaded scenarios indicate the scenarios chosen for illustration in figures 3, 4, 6, 7 and 8, and the baseline scenario.

Formateret: Normal, Indrykning: Venstre: 0,63 cm, Ingen punkttegn eller nummerering

formaterede: Skrifttype: Calibri, Fed, Skriftfarve: Tekst 1, Dansk, Knibning med 12 pkt

Formateret: Ingen punkttegn eller nummerering

4 Results

4.1 ~~DAISY and MIKE SHE~~ M~~m~~odel evaluation

The first phase of the calibration scheme was the MIKE SHE model calibration. A detailed presentation and evaluation of the water quantity performance of MIKE SHE ~~and DAISY~~, have previously been described in Karlsson et al. (2014) and Karlsson et al. (2016). MIKE SHE was reported to have good performance in the calibration ~~(~~and validation periods (Figure S1)~~)~~ with water balance error of 3% during calibration and ~~(~~6/-10% in the validation periods~~)~~; and RMSE value of 1.5 m^{3}/s in the calibration period and ~~(~~1.2/-1.5 m^{3}/s during validation~~)~~ for the main station.

The second phase of the calibration scheme was the calibration of Daisy. Due to the complicated setup with manual simultaneous calibration of more than 12.000 1D DAISY models, the water balance performance of the DAISY model was reported to be somewhat poorer with water balance errors of 16% in the calibration period and 3- 23% in the validation periods. The water quantity performance of DAISY is also described in more detail in Karlsson et al. (2016). The results from the subsequent manual calibration of the nitrate leaching in DAISY using the N yields for the region, can be seen in Table 3~~Table 2~~. For all the crops in the region the DAISY model is able to reproduce the observed harvested N within a margin of 0-5 kg harvested N/ha. The DAISY model is therefore able to represent the observed values of nitrate yields to a satisfactory level on catchment scale. The catchment average root zone leaching from Daisy was 40 kg NO3-N/ha/year; as there are not direct measurement of leaching, this value cannot be directly verified. But Hansen et al. (2018) have reported values in the same order of magnitude (35.1 kg NO3-N/ha/year) for a different time period (2000-2010) using the NLES leaching model (Kristensen et al., 2003; Kristensen et al., 2008), while Højberg et al. (2017); Højberg et al. (2015a) reported values of 37.5 kg NO3-N/ha/year.

~~The results from the subsequent manual calibration of the nitrate leaching in DAISY using the N yields for the region, can be seen in Table 2. For all the crops in the region the DAISY model is able to reproduce the observed harvested N within a margin of 0-5 kg harvested N/ha. The DAISY model is therefore able to represent the observed trends in nitrate yields to a satisfactory level on catchment scale.~~

Formateret: Normal, Mellemrum Før: 0 pkt., Efter: 0 pkt., Linjeafstand: enkelt, Hold ikke linjer sammen

formaterede: Skrifttype: Ikke Fed

formaterede: Skrifttype: Ikke Fed

formaterede: Skrifttype: Ikke Fed

Table 32: Observed and simulated harvested N in kg N/ha for the crop type on Funen during the calibration period 2004-2007. Grain type crops are stated as harvested N in the grain, while the remaining crops are calculated as total harvested dry matter.

Crop	Observed harvested kg N/ha	Simulated harvested kg N/ha
Spring barley	101	102
Winter wheat	122	124
Winter rape	105	107
Silage maize	151	152
Grass in rotation	258	259
Grass permanent	78	83
Sugar beets	179	179
Grain maize	No data	-

The third and final phases of the calibration is the calibration of the nitrate model or the calibration of the redox interface depth using the observed nitrate arrival percentage (NAP). ~~Baseline nitrate reduction map~~

The observed ~~nitrate arrival percentage (NAP)~~NAP of the catchment was estimated to 35-39%. The span is a result of the choice of time period; however, a NAP of 37% was selected as the final calibration target. Several different combinations of the migration constant (f) and the minimum redox depth (min.redoxdepth) resulted in a NAP of 37%. ~~To select the most appropriate combination, the cumulative distribution of the resulting redox depth of a given parameter combination is plotted against the distribution of observed redox depths.~~ The cumulative distribution of the redox depths for all combinations are ~~then~~ compared to the cumulative distribution of the observed redox depth ~~is both compared to the simulated values at the actual point of observational measurement as well as to the total fractional distribution of the whole catchment~~ (not shown), and the

parameter combination yielding the best representation of the fractional redox depth distribution is identified. Based on this analysis the best combination with the correct NAP was found to be f=0.01yr and min.redoxdepth=3m. Figure 2~~Figure 2~~ (left) shows the resulting depth to the redox interface for this combination. Generally, the depth to the redox interface is ~~fairly~~ shallow, with a mean depth of 4.0 meters (standard deviation of 5.6 m). This corresponds ~~fairly~~ well with the previously reported redox depth (Koch et al., 2019b). With the calibrated redox interface depth the resulting nitrate load in the river is 15 kg NO3-N/ha/year, this correspond well with the observed loading of approximately 14 kg NO_3-N/ha/year measured at Kratholm station.

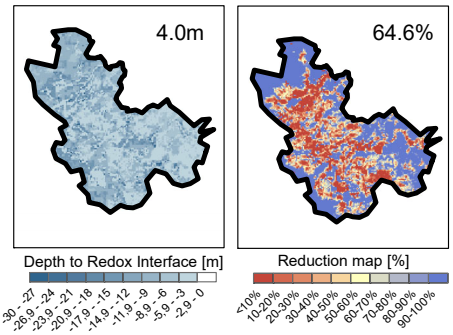

Figure 2: Left – Resulting depth to redox interface after calibration. Right - Nitrate reduction potential maps for the baseline scenario (Land use 0/observed climate), showing the fraction of the leached nitrate that are reduced for each grid. The number in the upper right corner of each panel is the average across all grids.

~~The baseline reduction map was generated based on the nitrate input from the DAISY model for the present period and the current land use (Figure 2, right). The mean N reduction fraction in the catchment is 65% with a standard deviation of 38% points. The spatial distribution on the map shows high reduction potentials in the uplands at the border of the model, likely where infiltrating water has a longer travel path to the river, and in areas where the redox interface is shallow. Lower reduction potential is seen in the areas near the stream network and lowland areas with deep redox interface.~~

Formateret: Normal, Linjeafstand: enkelt

4.2 Baseline, r~~R~~eference and future nitrate reduction map

The baseline reduction map was generated based on the nitrate input from the DAISY model for the present period and the current land use (Figure 2~~Figure 2~~, right). The mean nitrate reduction fraction in the catchment is 65% with a standard deviation of 38%. The spatial distribution on the map shows high reduction potentials in the uplands at the border of the model, likely where infiltrating water has a longer travel path to the river, and in areas where the redox interface is shallow. Lower reduction potential is seen in the areas near the stream network and lowland areas with deep redox interface.

Formateret: Normal, Ingen punkttegn eller nummerering

Utilizing the different nitrate input from the land use/climate model scenarios, 45 nitrate models (observational, reference and future, Table 2~~Table~~ ~~Table 2~~) were run with the calibrated redox interface. The depth to the redox interface is ergo assumed to be constant in time and is not updated for each scenario. This assumption is acceptable because of the slow migration of the interface, where the migration constant predicts one meters downward movement every 100 years. Following the procedure described in section 0, this generates 45 nitrate reduction potential maps. The statistics for all 45 reduction potential maps is shown in Table 4~~Table 3~~, and a selection of these reduction maps can be seen in ~~Figure S1~~Figure S2 (~~Figure 3~~Supplementary Material). ~~In the top row in Figure 3, the observed climate is used, changing only the land use (scenarios 2-5). In the bottom row the present land use (LU0) is used, while using future climate projected by the four climate models (scenarios 26, 31, 36 and 41).~~

Period	Climate	Land use (LU) scenario: Baseline	Agriculture for nature	Extensive agriculture	High-tech agriculture	Market driven agriculture
Control period, 1990-2099	Obs. Climate	1	2	3	4	5
	ECHAM5-HIRHAM5	6	7	8	9	10
	ECHAM5-RCA3	11	12	13	14	15
	ARPEGE-RM5.1	16	17	18	19	20
	HadCM3-HadRM3	21	22	23	24	25
Future period, 2080-2099	ECHAM5-HIRHAM5	26	27	28	29	30
	ECHAM5-RCA3	31	32	33	34	35
	ARPEGE-RM5.1	36	37	38	39	40
	HadCM3-HadRM3	41	42	43	44	45

Table 3: Land use and climate scenario matrix showing the scenario numbers.

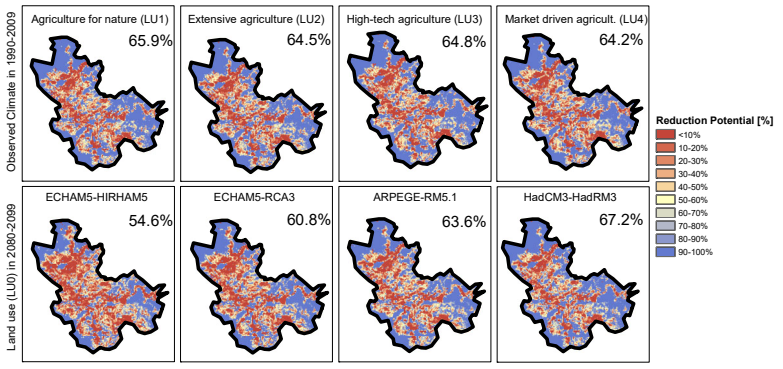

Figure 3: Nitrate reduction potential maps for four land use scenarios (LU1-4) in the observational period (top row) and four climate scenarios (LU0) for the future climate (bottom row), showing the fraction of the added nitrate that is reduced for each grid.

Formateret ... [1]
formaterede ... [2]
formaterede ... [4]
formaterede ... [5]
formaterede ... [6]
formaterede ... [7]
formaterede ... [8]
formaterede ... [9]
formaterede ... [10]
formaterede ... [11]
formaterede ... [12]
formaterede ... [13]
formaterede ... [3]
formaterede ... [14]
formaterede ... [15]
formaterede ... [16]
formaterede ... [17]
formaterede ... [18]
formaterede ... [19]
formaterede ... [20]
formaterede ... [21]
formaterede ... [22]
formaterede ... [23]
formaterede ... [24]
formaterede ... [25]
formaterede ... [26]
formaterede ... [27]
formaterede ... [28]
formaterede ... [30]
formaterede ... [31]
formaterede ... [32]
formaterede ... [33]
formaterede ... [34]
formaterede ... [29]
formaterede ... [35]
formaterede ... [36]
formaterede ... [37]
formaterede ... [38]
formaterede ... [39]
formaterede ... [40]
formaterede ... [41]
formaterede ... [42]
formaterede ... [43]
formaterede ... [44]
formaterede ... [45]
formaterede ... [46]
formaterede ... [47]
formaterede ... [48]
formaterede ... [49]
formaterede ... [50]

		Land use				
Period	Climate input	Baseline	LU1	LU2	LU3	LU4
Control period (1990-2009)	Obs. Climate	0.65 (0.38)	0.66 (0.38)	0.65 (0.38)	0.65 (0.38)	0.64 (0.37)
	ECHAM5–HIRHAM5	0.62 (0.38)	0.63 (0.38)	0.62 (0.38)	0.62 (0.38)	0.62 (0.38)
	ECHAM5–RCA3	0.65 (0.37)	0.66 (0.37)	0.65 (0.37)	0.65 (0.37)	0.64 (0.37)
	ARPEGE–RM5.1	0.69 (0.36)	0.70 (0.36)	0.69 (0.36)	0.68 (0.37)	0.68 (0.36)
	HadCM3–HadRM3	0.63 (0.38)	0.64 (0.38)	0.61 (0.38)	0.63 (0.38)	0.62 (0.38)
Far future (2080-2099)	ECHAM5–HIRHAM5	0.55 (0.38)	0.55 (0.39)	0.55 (0.38)	0.55 (0.39)	0.54 (0.38)
	ECHAM5–RCA3	0.61 (0.38)	0.62 (0.39)	0.61 (0.38)	0.61 (0.39)	0.60 (0.38)
	ARPEGE–RM5.1	0.64 (0.37)	0.64 (0.38)	0.64 (0.37)	0.63 (0.37)	0.63 (0.37)
	HadCM3–HadRM3	0.67 (0.37)	0.68 (0.37)	0.67 (0.37)	0.66 (0.37)	0.65 (0.37)

Table 4: Mean and standard deviation (in brackets) of nitrate reduction potential maps (proportion of nitrate N reduced).

All scenarios show similar patterns of reduction zones with high and low removal fractions when compared to the baseline scenario map (Figure 2~~Figure 2~~). However, although the general pattern of the reduction maps is comparable, there are spatial differences between the maps. The redox depth remains constant and all nitrate crossing this interface are assumed to be reduced, regardless of amount. Therefore, the reason for these changes in the nitrate reduction potential map results from changes in the flow path and/or changes in nitrate ~~N~~ input from Daisy, reflected in differences between drain/interflow versus groundwater flow to streams, and timing of nitrate release from the root zone.

~~To investigate to what degree land use changes and climate change affect the reduction map, the difference between these scenarios and the reference scenario is shown in Figure 4.~~

Feltkode ændret

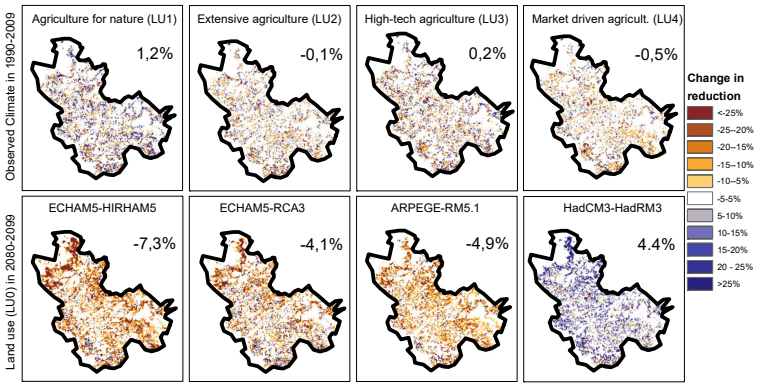

Figure 34: Difference in nitrate reduction potential maps between: Top row - Four land use scenarios LU1-4 (Scenario 2-5) and the baseline scenario with land use 0 (Scenario 1). Bottom row: The four future climate model scenarios (scenarios 26, 31, 36, 41) and the reduction maps for the corresponding climate model reference period (scenarios 6, 11, 16, 21) all for land use 0.

4.3 Impact of land use change on reduction maps

~~To investigate to what degree land use changes and climate change affect the reduction map, the difference between these scenarios and the reference scenario is shown in Figure 4.~~

To investigate the impact of land use change on the reduction maps, only land use is changed while climate remains constant, shown as the difference between land use changes scenarios and the baseline scenario (Figure 3~~Figure 4~~, top row). The water balance of the models, and hence the groundwater level and water flow paths, are affected mainly by a possible change in evapotranspiration that is introduced with new crop rotation systems and vegetation types. Drains are still present in the entire catchment regardless of land use and are only active when they are required (submerged below the groundwater table). At the same time, the land use changes result in a nitrate input distribution and timing that may differ from the current land use (LU0). The changes are minor and give both higher and lower reduction potential, depending on changes in land use and vegetation for the individual grids (Figure 4, top row).

Formateret: Normal, Ingen punkttegn eller nummerering

Formateret: Tabulatorstop: 3,34 cm, Venstre

The changes in the average catchment water flow components as a result of land use change is shown in Figure 4~~Figure 5~~, left. This shows the change of each component, drain flow, overland flow and base flow, when changing from a scenario run with land use 0 to the scenarios with land use 1-4. These changes minor for the overall water balance on the catchment scale for all land use change scenarios (Figure 5, left) .

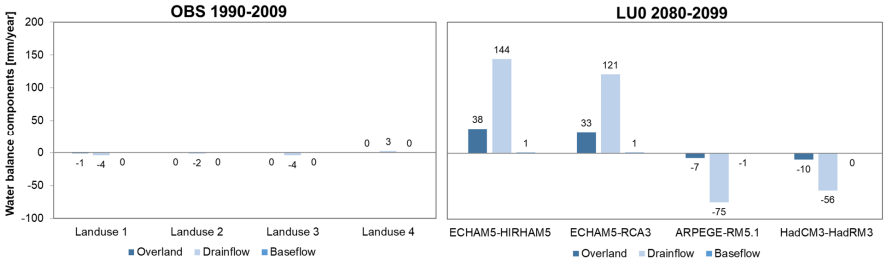

Figure 4~~5~~: The change in the distribution of the water balance components in mm/year caused by changes in land use and climate change. Left – The difference for the four land use scenarios LU1-4 (Scenario 2-5) and the baseline scenario with land use 0 (scenario 1). Right: The difference between the four future climate model scenarios (scenarios 26, 31, 36, 41) and the corresponding climate model reference period (scenarios 6, 11, 16, 21) all for land use 0 (modified from Karlsson et al. (2016)).

The drain flow component is a primary conductor for non-reduced nitrate, because it represents fast and shallow flows above the redox interface. It is therefore relevant to look at the spatial distribution of the changes in drain flow for the scenarios. While the bias corrections ensure that the climate models reproduce the overall mean and variances of the observed climate, they do not necessarily ensure consistency in the temporal structure of precipitation. Hence, the overall net precipitation (precipitation-actual evapotranspiration) may change slightly across the climate models, and we have therefore plotted the change in drain flow fraction (Figure 5~~Figure 6~~), defined as the drain flow divided by net precipitation, instead of the drain flow component itself. As for the changes in the reduction map (Figure 3~~Figure 4~~), the differences between the reference and land use scenario drain flow fractions, are very small and sporadic. The same is found for changes in recharge and groundwater head presented in ~~Figure 7~~~~Figure S2~~Figure S3 and ~~Figure 8~~~~Figure S3~~Figure S4 (top row, Supplementary material). Averaged across the catchment, the change in land use gives rise to a maximum 1.2% change in reduction potential (Figure 4). For all

45 runs, the general statistics also show that changing the land use (horizontally, Table 4~~Table 3~~) does not change the mean reduction potential more than a maximum of ±2%.

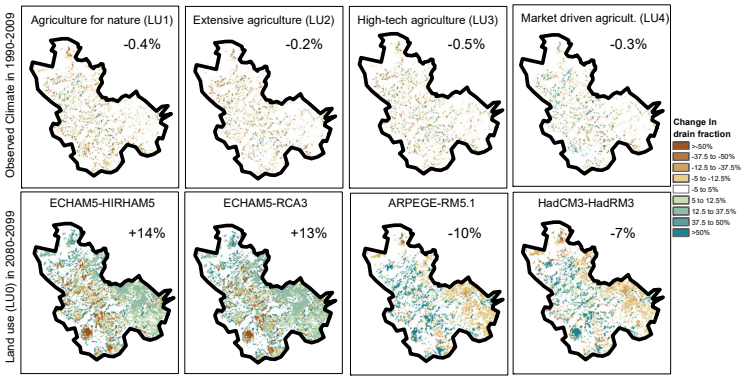

Figure 56: Changes in the drain flow fraction from baseline (LU0) to the four land use scenarios (LU1-4) in the observational period (top row) and from the reference period to the future period for four climate models using LU0 (bottom row). Drain flow fraction is defined as drain flow divided by net precipitation. Green colors indicate that a larger percentage of the net precipitation is channeled into the drains for the future. Number in upper right corner indicate the relative change in drain flow fraction from reference period to future period. The corresponding percentage of drain flow in the baseline scenario is 31%.

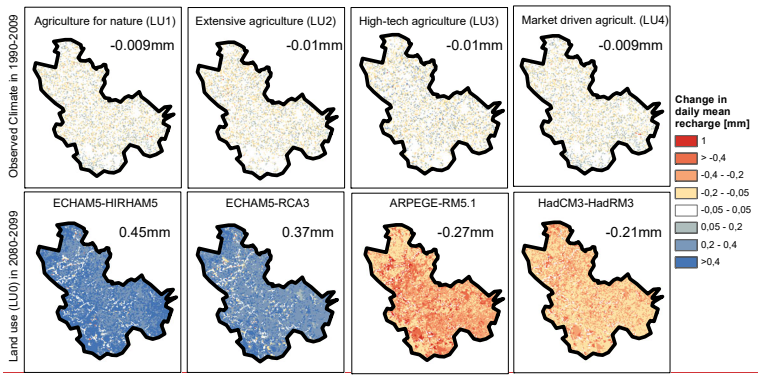

~~Figure 7: Changes in daily recharge from baseline (LU0) to the four land use scenarios (LU1-4) in the observational period (top row) and the change for four climate scenarios (LU0) from reference to future period (bottom row).~~

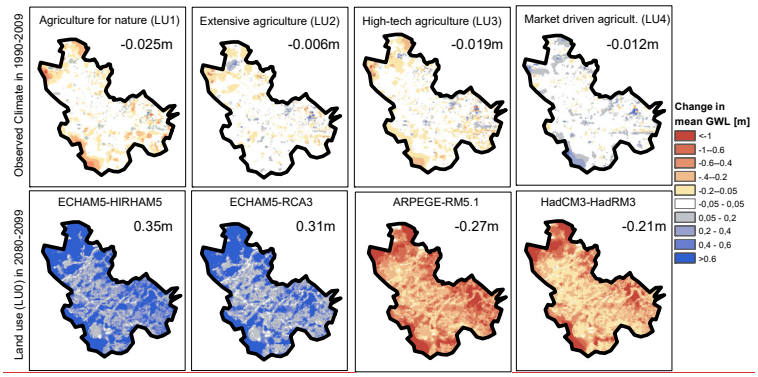

~~Figure 8: Changes in groundwater level from the upper saturated layer. Changes are reported as change from (LU0) to LU1-4 with observational climate for the top row and from RCM reference period to RCM future period for the bottom row. Figure modified from Karlsson et al. (2016).~~

4.4 Impact of land use and climate change ~~impact~~ on reduction maps

Figure 3~~Figure 4~~, bottom row, shows the results for the future climate compared to the corresponding reference period. For the future simulations, not only the water flow paths are affected by the change in amount and distribution of net precipitation, but also the vegetation uptake is considerably different due to increasing potential evapotranspiration. The impact of these changes is evaluated in Figure 4~~Figure 5~~, right, where the changes in the flow components are shown from the reference to the future period. The climate model projections have important impacts on the distribution of the water balance components and substantial differences are found among the models. Even if land use remains constant, the timing and amount of nitrate leakage are subject to significant variations as a result of climate changes. For the reduction maps (Figure 3~~Figure 4~~), these changes results in larger differences when compared to the maps produced for the reference period. Averaged across the catchment, changes of up to 7.3% ~~point~~ p.p. are recorded for the four scenarios and for all 45 scenarios the change is up to ±8%.

From a water balance perspective, the four future climate model projections vary greatly, but may be grouped in two overall categories. The first category includes the wet models, ECHAM5-HIRHAM5 and ECHAM5-RCA3 (Table 1~~Table 1~~). Both show a small decrease in annual reference evapotranspiration. At the same time precipitation is projected to increase in all seasons resulting in an annual increase of 15 – 30%. As a result, the net precipitation (Figure 4~~Figure 5~~) and groundwater recharge (~~Figure 7~~~~Figure S2~~Figure S3) increase considerably. Since there is a limit to how fast water can be pushed through the deeper groundwater systems, the fast flow components (overland, drain flow) both increase substantially.

Even though the drain flow produced with the wet climate model projections generally increases, the drain flow fraction, defined as the drain flow divided by net precipitation (Figure 5~~Figure 6~~) shows two overall signals. In the eastern uphill area, the change in drain flow fractions are positive, while in the central and western areas, in the river valleys, the change in drain fraction is negative. This implies that less net precipitation, relatively, is channeled through the drainage system than in the reference period in the river valleys (brown areas), while relatively more net precipitation is captured by drains in the eastern uphill locations. This highlights how the change in the distribution of the flow components also changes the spatial pattern across the catchment. The underlying explanation for the pattern recognized in the wet models, is primarily found as a moderate increase in upwelling water to the drainage system in the lowlands in the future compared to the substantial increase in drainage in the uphill areas.

The increase in groundwater recharge (~~Figure 7~~~~Figure S2~~Figure S3) results in increasing groundwater levels (~~Figure 8~~~~Figure S3~~Figure S4). However, the change varies across the catchment and since flow is controlled by the gradient in hydraulic head, the non-homogeneous changes in heads will result in changes in flow direction. The general tendency is that groundwater levels increase most in the upstream parts of the catchment, while it remains the same in the valleys near the stream. Hence, the gradients will become steeper, which results in an increase in the ratio of horizontal to vertical flow. Thus, this promotes near-surface flow paths in the subsurface.

As the fast flow components, like drain and overland flow, mainly carry non-reduced water, and the subsurface reduction depends on water being transported below the redox interface for nitrate reduction to take place, both the increase in fast flow components and the shallower flow paths for the infiltrated water, is expected to give rise to a lower reduction potential as is indeed observed in Figure 3~~Figure 4~~ and Table 4~~Table 3~~.

The second climate model category (dry models) includes ARPEGE-RM5.1 and HadCM3-HadRM3 (Table 1~~Table 1~~), that both show a significant increase in annual reference evapotranspiration of 10-20% (Karlsson et al., 2016). With respect to precipitation, the two models show a slight decrease or no change in annual values, whereas lower precipitation is found during summer and autumn for both models. Therefore, net precipitation decreases for both models, leading to a decrease in the fast flow components (overland, drain flow) for the future projections (Figure 4~~Figure 5~~). The reduction in net precipitation also results in a reversal of the distribution of the drain flow fraction (Figure 5~~Figure 6~~) and a decreasing groundwater recharge (~~Figure 7~~~~Figure S2~~Figure S3).

These changes are reflected in the spatial distribution of the change in groundwater level (~~Figure 8~~~~Figure S3~~Figure S4). As found for the wet models, the general tendency is that groundwater levels change more in the upstream parts of the catchment compared to the valleys near the stream. Therefore, the gradients will become less steep, resulting in a decrease in the ratio of horizontal to vertical flow. This leads to a higher degree of slower and deeper groundwater flow paths, and potentially, to more nitrate crossing the redox interface.

The decrease in fast flow components and the deeper flow path supports the fact that the two models project higher reduction potential in the future. This is ~~also~~ indeed found for one of the models, HadCM3-HadRM3, which generally has the largest increase in reduction potential of the four models, from the average reduction of 63% in the reference to 67% in the future simulation (LU0, Figure 3~~Figure 4~~ and Table 4~~Table 3~~).

However, the other model, ARPEGE-RM5.1, shows a complete opposite signal with lower reduction potential (Figure 3~~Figure 4~~). Initially, this anomaly did not seem to be explainable by changing flow paths as the changes (Figure 4~~Figure 5~~, ~~Figure 7~~~~Figure S2~~Figure S3 and ~~Figure 8~~~~Figure S3~~Figure S4) are very similar to the other dry model. However, as mentioned previously, changes in the timing and quantities of the nitrate root zone leakage from Daisy is also a determining factor for the reduction map, and these dynamics are not always apparent on average maps like the ones shown in Figure 3~~Figure 4~~, Figure 4~~Figure 5~~, ~~Figure 7~~~~Figure S2~~Figure S3 and ~~Figure 8~~~~Figure S3~~Figure S4. A closer inspection of the monthly changes in flow components and nitrate leakage provides a possible explanation for this phenomenon (calculations not shown).

The ARPEGE-RM5.1 model shows the absolute largest increase in nitrate leakage in January. Even though the model is generally dry, the January precipitation is projected to increase in the future. The dynamics in the model shows a shift in flow components for this month towards a smaller amount of drain flow and recharge, while overland flow increases, probably as a result of larger prolonged rainfall events. This shift combined with the very large increase in nitrate leakage leads to more non-reduced water in the system for the future period than for the control period. As this combination of larger nitrate leakage and flow components shifts are not seen in the HadCM3-HadRM3 model, it is, most likely, a result of the lower reduction potential for ARPEGE-RM5.1 in the future in spite of the overall drying signal from the model.

4.5 Effect on the nitrate flux using different reduction maps

To evaluate the impacts of using a fixed reduction map versus different maps calculated for each scenario explicitly considering differences caused by changes in land use and climate change, the total catchment nitrate load (nitrate arrival at Kratholm) were calculated using two different approaches for all scenarios:

1. A fixed reduction map (the baseline reduction map) is used and combined with projected nitrate leaching from the root zone.
2. Targeted reduction maps, i.e. different reduction maps for each scenario (as calculated above) are used and combined with projected nitrate leaching from the root zone.

For both approaches nitrate arrival is calculated for the observational, reference and future periods. The resulting nitrate arrivals for approach 2 is then for each case compared to the corresponding scenario in approach 1; thereby illustrating the effect of using a targeted reduction map compared to a baseline reduction map (Figure 6~~Figure 9~~).

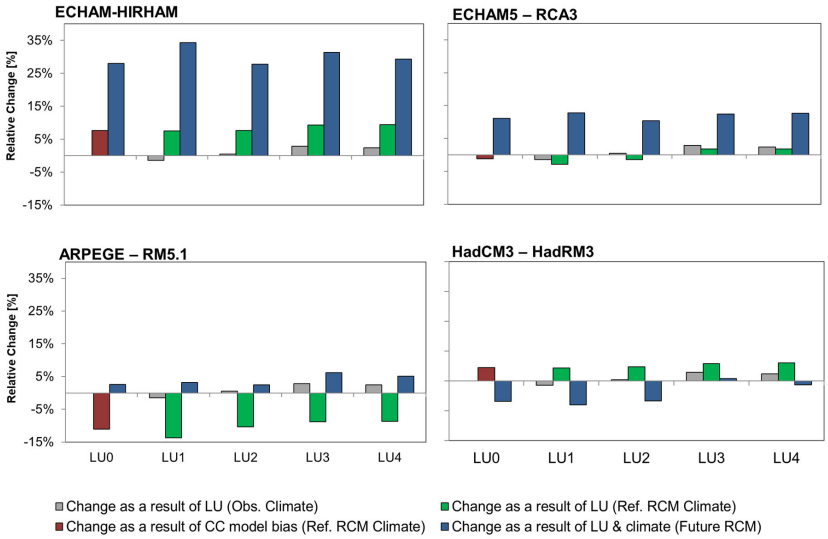

Figure 6~~9~~: Bars denote the change in nitrate flux at the catchment outlet that arises from using either a fixed ~~the baseline~~ nitrate reduction potential map (baseline) or using a ~~the~~ reduction map based on the individual~~from the~~ scenario~~s~~. The scenarios encompass cases with different land use (grey), climate model data for the present (red bar) with land use changes (green bars) or future climate data and land use changes (blue bars).

The grey bars in Figure 9 show the relative change (compared to baseline), when applying targeted reduction maps for the four land use scenarios, but using observed climate. Note therefore that the grey bars are the same for all four plots. The effect of the targeted reduction maps versus the fixed reduction map manifests in only limited spread in the estimated nitrate arrivals by only 1% - 3%. This implies that for a case of changing land use, the fixed reduction map is a reasonable approximation of the reduction potential in the catchment.

The green bars in Figure 9 represents the same effect as for the grey bars (targeted versus fixed reduction maps); however, here the climate is the reference climate for each of the four climate models. For all models, the effect is here larger than using the observed climate. This phenomenon is mainly due to the inherent bias of the reference climate model simulations. This becomes clear when looking at the first bars of each plot (red bars), denoting the change when only observed climate is replaced by reference climate but maintaining the current land use setup (LU0). Even though the climate model output is bias corrected such that the general statistics in the reference period resembles those of the observations, there may still be differences in the temporal structure of the climate model outputs, which may impact hydrological simulations. This is an important issue to bear in mind when analyzing the future signal presented by the blue bars. However, the effect of land use can still be approximated by comparing the results from LU0 to LU1-4 for the different climate models. Again, the magnitude of the effect is between 1% - 3% change in nitrate arrival; however, the models do not agree on which land use causes the largest change (being either LU1 or LU4).

For the blue bars the differences from the fixed reduction map to targeted reduction maps become a combination of bias correction limitations, land use change and climate change. Even though it is not possible to completely separate the signal of these three components, a cautious estimation can again be achieved by ~~comparing~~ subtracting the blue bars with~~to~~ the red bar result~~s~~ from LU0 in the reference period ~~(red bars)~~, so that the signal from the climate model bias is tried to be removed. For a dry model like ARPEGE-RM5.1 the effect (land use and climate) on the nitrate arrival is in the range of -5% to -9%, while for HadCM3-HadRM3, it is between -4% to 4%. The largest effects are found for the wet models, with changes ranging from 20% - 27% for ECHAM-HIRHAM, followed by ECHAM-RCA3 with 9% - 12%. This shows that the consequences of using a fixed reduction map may be considerable, in particular with large changes in climatic conditions.

5 Discussion ~~and conclusions~~

5.1 Nitrate ~~-~~reduction maps are not constant in time

Our analysis clearly demonstrates that nitrate ~~N~~ reduction maps are a result of complicated interactions between climate, vegetation, geology and farm management leading to a diversity of potential nitrate inputs, distributions, timing, flow paths and reduction capability. This implies that nitrate ~~N~~ reduction maps calculated for present climatic conditions and flow patterns will differ from nitrate ~~N~~ reduction maps under future climate and land use conditions. The main factor causing this is differences in the precipitation/evapotranspiration regime that results in differences in how large a fraction of the water percolating from the root zone reaches the stream via shallow flow routes above the redox interface, such as overland flow and runoff via drain pipes, and how large a fraction that takes a route through deeper groundwater zones and crosses the redox interface. Therefore, ~~N-reduction maps~~ nNitrate reduction maps also differ between a wet year and a dry year in the present climate.

Compared to climate effects, the impacts of land use change are minor, because land use change does not affect the flow regime to the same extent as variability and change in climate. This novel finding has not been recognized in previous studies of ~~N-reduction maps~~ nNitrate reduction maps such as Hansen et al. (2014b), Højberg et al. (2015), Andersen et al. (2016) and Refsgaard et al. (2019). Nevertheless, it is important to note that the distribution of drains in the catchment was not changed during the land use change scenarios. Hence, uniform drain distribution and parameterization are assumed, where the drainage component covers both natural (ditches and small canals) and agricultural drains. However, a different approach could have been adopted in the land use change scenarios by changing the drainage efficiency (by adjusting drainage parameters) in re- or deforested areas. Unfortunately, little information is available to guide this fine-tuning. However, the influence of land use change on the water balance and therefore the nitrate reduction is expected to increase if this effect is accounted for.

To encapsulate the ~~full~~ range of uncertainty and influences from climate and land use scenarios in this setup; all scenario combinations were used. However, ~~it is also worth noting, that~~one could speculate that not all combinations of land use and climate change scenarios may ~~not~~ be equally likely or ~~even~~ plausible in the future, as~~. This is because~~ decisions on land use

application made by local farmers or through national regulations are made concurrently to adapt or mitigate changes in the climatic conditions.

The present study was carried out for a groundwater dominated catchment characterized by till deposits, confined aquifers, and relatively shallow redox interfaces and phreatic groundwater tables. We consider the conclusions to be applicable to catchments with similar hydrogeological conditions, while they cannot be used in groundwater dominated catchments characterized by alluvial plains without fast flow components such as overland flow and drainpipe/ditch flow and aerobic groundwater systems without a redox-interface. Similarly, the conclusions cannot be transferred to surface water dominated catchments, where the nitrate ~~N~~ reduction takes place in streams and lakes, although we suspect that non-linearities may cause similar effects here.

In this study the location of redox interface was assumed to be the same for both present and future scenarios. While this assumption may be reasonable in relation to the slow natural migration of the redox interface caused by percolation of oxygen, the redox interface migration may be escalated by nitrate application on the land surface as reported by e.g. Böhlke et al. (2002) and Wriedt and Rode (2006). This issue cannot be addressed within the framework of this study, but the effect on the redox interface may be substantial especially for land use scenarios with high nitrate application.

5.2 Water management implications

The advantages of assuming a fixed reduction map ~~is~~are that any projected nitrate input, regardless of climate and land use scenario, can be multiplied with the reduction map and thus provide a projected nitrate outflow estimate with little effort and time spent. However, as is shown in the present study, the assumption that the reduction map is constant in a changing environment is problematic. The good question then is how large errors are made by assuming a fixed reduction map and how should this be dealt with in water management practices.

The analysis indicates that assuming fixed reduction maps leads to small errors when dealing with land use change impacts but may lead to substantial errors (up to 10% on catchment ~~N~~ nitrate load) when climate change projections are included.

Land use change impacts may however be underestimated as a result of the uniform drainage setup. 10% error on the reduction map may potentially have major impacts on practical water management. -Considering for instance the baseline scenario in Table 4, where the average N-reductions vary between 55% and 67% reduction, this implies that the net impact of a 100 kg N reduction in leaching from the root zone will vary between 45 kg and 33 kg (i.e. 30%). Such changes are larger than the effects of sophisticated mitigation measures (Hansen et al., 2017). Whether such errors are acceptable depends on the purpose and context in specific water management situations. Thus, using fixed reduction maps may well be justifiable for initial screening purposes, while targeted reduction maps, explicitly calculated for specific scenarios, may be required for design of remediation measures having significant socio-economic impacts for stakeholders. The uncertainty of using a fixed reduction map for future scenarios ~~Such effects~~ should of course be seen in the context of the inherent uncertainties of the nitrate reduction maps (Hansen et al., 2014b).

The indication that errors can be up to 10% is based on only a single case study with one catchment, one model and a limited number of land use and climate change scenarios. While similar results may be found when applying the same approach for catchments governed by the same dominant flow processes and land use types, like the one investigated in this study. The error must be expected to~~will~~ be site and context specific and therefore causes projection uncertainties that should be addressed along with other known sources of uncertainty such as climate model projections, land use projections, parameter uncertainties, geological uncertainty, and hydrological model structural uncertainty ~~(~~(Hansen et al., 2014b; Karlsson et al., 2016). ~~Karlsson et al., 2016).~~ Furthermore, during calibration and setup of the model assumptions must be made, adding to the uncertainty. Parameter estimation are here done in a stepwise fashion, and the catchment scale calibration of Daisy along with a particle tracking approach limits the evaluation of performance of the nitrate component to mean catchment figures, and the dynamic of the nitrate system is thus impossible to verify. To account for this a full solute transport solution would be necessary but was unfortunately not possible in the framework of this study; but would be a relevant next step in investigating uncertainties and improve model verification.

6 Conclusions

Nitrate reduction maps are valuable tools used for calculation of remediation and climate change effects on nitrate leaching, and are generally considered constant in time, even though the timing of nitrate leaching, and flow paths may change. In this study we investigate the potential consequence for estimation nitrate climate and land use change impact projections when assuming a fixed reduction map. For an agricultural dominated catchment in Denmark, the Daisy model was used to provide nitrate leaching input, while the hydrological model Mike She was used to simulate the flow regime and nitrate flow path through particle tracking. Four land use scenarios and four climate change projections were evaluated. The main finding of the study was:

- Changing climate conditions lead to reduction map changes of up to 10%; whilst effects from land use changes where minor. However, land use effects may be underestimated due to drainage formulations in non-agricultural areas.
- Thus, the uncertainty of the reduction maps is dependent on both model setup and assumptions, the catchment flow regime as well as affected by the span of the chosen land use and climate change scenarios.
- The error will therefore be specific for the study site and context and it should, consequently, be tackled along with other sources of uncertainty, like geological, parameter, and model structure uncertainties that are not evaluated in this study.

Formateret: Linjeafstand: Dobbelt

Formateret: Normal, Mellemrum Før: 0 pkt., Linjeafstand: enkelt, Ingen punkttegn eller nummerering, Hold ikke linjer sammen

Author contributions

IKS performed model simulations, wrote part of the paper and produced figures. TSO and JCR contributed to formulation of the conceptualization, methodology and simulation assistance, as well as the writing of the paper. DT, CDB and JEO contributed to the methodology and the writing of the paper. CDB and JEO additionally provided input data and results for the paper.

Competing interests.

The authors declare that they have no conflict of interest.

Data/code availability

The hydrological model is based on the commercial software MIKE SHE and therefore model code is not available.

Data from the study is available upon request and through the public server at https://dataverse01.geus.dk. An exception to this is the observed climate data input which is ~~owned by~~currently the property of the Danish Meteorological Institute (DMI), but will be made publicly available through https://www.dmi.dk/frie-data/ before end of 2023. ~~.~~

Acknowledgements

The present study was funded by a grant from the Danish Strategic Research Council for the Centre for Regional Change in the Earth System (CRES – www.cres-centre.dk) under contract no: DSF-EnMi 09-066868.

References

~~Abbott, M.B., Bathurst, J.C., Cunge, J.A., O'Connell, P.E., Rasmussen, J., 1986. An introduction to the European hydrological system – systeme hydrologique europeen, "She", 2: Structure of a physically-based, distributed modeling system. Journal of Hydrology, 87: 61-77.~~

~~Abrahamsen, P., Hansen, S., 2000. Daisy: an open soil-crop-atmosphere system model. Environmental modelling & software, 15(3): 313-330.~~

~~Allen, R.G., Pereira, L.S., Raes, D., Smith, M., 1998. Crop evapotranspiration - Guidelines for computing crop water requirements, FAO - Food and Agriculture Organization of the United Nations, Rome, Italy.~~

~~Andersen, H.E. et al., 2016. Identifying Hot Spots of Agricultural Nitrogen Loss Within the Baltic Sea Drainage Basin. Water, Air, & Soil Pollution, 227(1): 38. DOI:10.1007/s11270-015-2733-7~~

~~Böhlke, J.K., Wanty, R., Tuttle, M., Delin, G., Landon, M., 2002. Denitrification in the recharge area and discharge area of a transient agricultural nitrate plume in a glacial outwash sand aquifer, Minnesota. Water Resources Research, 38(7): 10-1-10-26. DOI:10.1029/2001WR000663~~

~~Børgesen, C.D. et al., 2013. Udviklingen i kvælstofudvaskning of næringsstofoverskud fra dansk landbrug for perioden 2007-2011. Evaluering af implementerede virkemidler til reduktion af kvælstofudvaskning samt en fremskrivning af planlagte virkemidlers effekt frem til 2015, DCA - Nationalt Center for Fødevarer og Jordbrug, Tjele, Denmark.~~

~~Børgesen, C.D., Olesen, J.E., 2011. A probabilistic assessment of climate change impacts on yield and nitrogen leaching from winter wheat in Denmark. Natural Hazards and Earth System Sciences, 11(9): 2541-2553. DOI:10.5194/nhess-11-2541-2011~~

~~DHI, 2019. User Guide, DHI – Water & Environment, Hørsholm, Denmark.~~

Diaz, R.J., Rosenberg, R., 2008. Spreading dead zones and consequences for marine ecosystems. Science, 321(5891): 926-9. DOI:10.1126/science.1156401

Ernstsen, V.H., A.L., Jakobsen, P.R., von Platen,, F., T., L, Hansen, J.R., Blicher-Mathiasen, G.,, Bøgestrand, J., Børgesen, C.D., , 2006. Beregning af nitratreduktionsfaktorer for zonen mellem rodzonen og frem til vandløbet. Data og metode for 1. generationskortet. , Danmarks og Grønlands Geologiske Undersøgelse, Copenhagen, Denmark.

Graham, D.N., Butts, M.B., 2005. Flexible, integrated watershed modelling with MIKE SHE. In: Singh, V.P., Frevert, D.K. (Eds.), Watershed Models, pp. 245-272.

Greve, M.H. et al., 2007. Generating a Danish raster-based topsoil property map combining choropleth maps and point information. Geografisk Tidsskrift, 107.

Hansen, A.L., Christensen, B.S.B., Ernstsen, V., He, X., Refsgaard, J.C., 2014a. A concept for estimating depth of the redox interface for catchment-scale nitrate modelling in a till area in Denmark. Hydrogeology Journal, 22(7): 1639-1655. DOI:10.1007/s10040-014-1152-y

Hansen, A.L., Gunderman, D., He, X., Refsgaard, J.C., 2014b. Uncertainty assessment of spatially distributed nitrate reduction potential in groundwater using multiple geological realizations. Journal of Hydrology, 519, Part A: 225-237. DOI:http://dx.doi.org/10.1016/j.jhydrol.2014.07.013

Hansen, A.L., Refsgaard, J.C., Olesen, J.E., Børgesen, C.D., 2017. Potential benefits of a spatially targeted regulation based on detailed N-reduction maps to decrease N-load from agriculture in a small groundwater dominated catchment. Science of The Total Environment, 595: 325-336. DOI:https://doi.org/10.1016/j.scitotenv.2017.03.114

Hansen, B., Dalgaard, T., Thorling, L., S£¿rensen, B., 2012. Regional analysis of groundwater nitrate concentrations and trends in Denmark in regard to agricultural influence. Biogeosciences Discussions. DOI:10.5194/bgd-9-5321-2012

Hansen, S., Jensen, H.E., Nielsen, N.E., Svendsen, H., 1991. Simulation of nitrogen dynamics and biomass production in winter wheat using the Danish simulation model DAISY. Fertilizer Research, 27(2-3): 245-259. DOI:10.1007/BF01051131

Højberg, A.L. et al., 2017. Review and assessment of nitrate reduction in groundwater in the Baltic Sea Basin. Journal of Hydrology: Regional Studies, 12: 50-68. DOI:https://doi.org/10.1016/j.ejrh.2017.04.001

Højberg, A.L. et al., 2015. En ny kvælstofmodel. Oplandsmodel til belastning og virkemidler. Metode rapport (A new nitrogen model. Catchment model for loads and measures. Methodology Report - In Danish). DOI:Available from http://www.geus.dk/DK/water-soil/water-cycle/Documents/national_kvaelstofmodel_metoderapport.pdf

Karlsson, I.B. et al., 2014. Significance of hydrological model choice and land use changes when doing climate change impact assessment. In: EGU (Ed.), EGU General Assembly 2014. Geophysical Research Abstracts, Wienna, Austria, pp. 1.

Karlsson, I.B. et al., 2016. Combined effects of climate models, hydrological model structures and land use scenarios on hydrological impacts of climate change. Journal of Hydrology, 535: 301-317. DOI:http://dx.doi.org/10.1016/j.jhydrol.2016.01.069

Karlsson, I.B., Sonnenborg, T.O., Seaby, L.P., Jensen, K.H., Refsgaard, J.C., 2015. The climate change impact of a high-end CO2-emission scenario on hydrology. Climate Research. DOI:doi: 10.3354/cr01265

formaterede: Engelsk (Storbritannien)

formaterede: Engelsk (USA)

Koch, J., Ernstsen, V., Højberg, A.L., 2019a. Dybden til redoxgrænsen, 100 m grid. In: (GEUS), D.N.G.U.f.D.o.G. (Ed.), Copenhagen, GEUS. DOI:https://data.geus.dk/geusmap/?mapname=denmark#baslay=baseMapDa&optlay=&extent=-139925.69284407864,5929490.944444444,1254925.6928440786,6520509.055555556&layers=redox_dybde_100m_grid

Koch, J. et al., 2019b. Modeling Depth of the Redox Interface at High Resolution at National Scale Using Random Forest and Residual Gaussian Simulation. 55(2): 1451-1469. DOI:10.1029/2018wr023939

Kristensen, K.J., Jensen, S.E., 1975. A Model for Estimating Actual Evapotranspiration from Potential Evapotranspiration. Hydrology Research, 6: 170-188.

Kunkel, R., Eisele, M., Schäfer, W., Tetzlaff, B., Wendland, F., 2008. Planning and implementation of nitrogen reduction measures in catchment areas based on a determination and ranking of target areas. Desalination, 226(1): 1-12. DOI:https://doi.org/10.1016/j.desal.2007.01.231

Madsen, H., 2000. Automatic calibration of a conceptual rainfall-runoff model using multiple objectives. Journal of Hydrology, 235: 276-288. DOI:10.1016/S0022-1694(00)00279-1

Merz, C., Steidl, J., Dannowski, R., 2009. Parameterization and regionalization of redox based denitrification for GIS-embedded nitrate transport modeling in Pleistocene aquifer systems. Environ Geol, 58(7): 1587-1599. DOI:10.1007/s00254-008-1665-6

Møller, J. et al., 2005. Fodermiddeltabel - Sammensætning og foderværdi af fodermidler til kvæg. 64.

Olesen, J.E. et al., 2019. Nitrate leaching losses from two Baltic Sea catchments under scenarios of changes in land use, land management and climate. Ambio, 48(11): 1252-1263. DOI:10.1007/s13280-019-01254-2

Olesen, J.E. et al., 2014. Scenarier for fremtidens arealanvendelse i Danmark. Vand og Jord, 21(3): 126-129.

Postma, D., Boesen, C., Kristiansen, H., Larsen, F., 1991. Nitrate Reduction in an Unconfined Sandy Aquifer: Water Chemistry, Reduction Processes, and Geochemical Modeling. Water Resources Research, 27(8): 2027-2045. DOI:10.1029/91wr00989

Refsgaard, J.C. et al., 2019. Spatially differentiated regulation: Can it save the Baltic Sea from excessive N loads? Ambio, 48(11): 1278-1289. DOI:10.1007/s13280-019-01195-w

Reusch, T.B.H. et al., 2018. The Baltic Sea as a time machine for the future coastal ocean. Science Advances, 4(5): eaar8195. DOI:10.1126/sciadv.aar8195

Seaby, L.P. et al., 2013. Assessment of robustness and significance of climate change signals for an ensemble of distribution-based scaled climate projections. Journal of Hydrology, 486: 479-493.

Statistikbanken, 2015. Statistical regional registrated annual mean yields. (In Danish) https://www.statistikbanken.dk/jord3.

Styczen, M. et al., 2004. Standardopstillinger til Daisy-modellen. Vejledning og baggrund, Institut for Vand og Miljø, DHI.

Trolle, D. et al., 2019. Effects of changes in land use and climate on aquatic ecosystems: Coupling of models and decomposition of uncertainties. Science of The Total Environment, 657: 627-633. DOI:https://doi.org/10.1016/j.scitotenv.2018.12.055

formaterede: Engelsk (USA)

formaterede: Engelsk (USA)

van Genuchten, M.T., 1980. A Closed-form Equation for Predicting the Hydraulic Conductivity of Unsaturated Soils. 44(5): 892-898. DOI:10.2136/sssaj1980.03615995004400050002x

van Vuuren, D.P. et al., 2011. The representative concentration pathways: an overview. Climatic Change, 109(1): 5. DOI:10.1007/s10584-011-0148-z

Wriedt, G., Rode, M., 2006. Modelling nitrate transport and turnover in a lowland catchment system. Journal of Hydrology, 328(1-2): 157-176. DOI:http://dx.doi.org/10.1016/j.jhydrol.2005.12.017

Wulff, F. et al., 2014. Reduction of Baltic Sea Nutrient Inputs and Allocation of Abatement Costs Within the Baltic Sea Catchment. AMBIO, 43(1): 11-25. DOI:10.1007/s13280-013-0484-5

Abbott, M.B., Bathurst, J.C., Cunge, J.A., O'Connell, P.E., Rasmussen, J., 1986. An introduction to the European hydrological system – systeme hydrologique europeen, "She", 2: Structure of a physically-based, distributed modeling system. Journal of Hydrology, 87: 61-77.

Abrahamsen, P., Hansen, S., 2000. Daisy: an open soil-crop-atmosphere system model. Environmental modelling & software, 15(3): 313-330.

Allen, R.G., Pereira, L.S., Raes, D., Smith, M., 1998. Crop evapotranspiration - Guidelines for computing crop water requirements, FAO - Food and Agriculture Organization of the United Nations, Rome, Italy.

Andersen, H.E. et al., 2016. Identifying Hot Spots of Agricultural Nitrogen Loss Within the Baltic Sea Drainage Basin. Water, Air, & Soil Pollution, 227(1): 38. DOI:10.1007/s11270-015-2733-7

Bruun, S., Christensen, B.T., Hansen, E.M., Magid, J., Jensen, L.S., 2003. Calibration and validation of the soil organic matter dynamics of the Daisy model with data from the Askov long-term experiments. Soil Biology and Biochemistry, 35(1): 67-76. DOI:http://dx.doi.org/10.1016/S0038-0717(02)00237-7

Böhlke, J.K., Wanty, R., Tuttle, M., Delin, G., Landon, M., 2002. Denitrification in the recharge area and discharge area of a transient agricultural nitrate plume in a glacial outwash sand aquifer, Minnesota. Water Resources Research, 38(7): 10-1-10-26. DOI:10.1029/2001WR000663

Børgesen, C.D. et al., 2013. Udviklingen i kvælstofudvaskning of næringsstofoverskud fra dansk landbrug for perioden 2007-2011. Evaluering af implementerede virkemidler til reduktion af kvælstofudvaskning samt en fremskrivning af planlagte virkemidlers effekt frem til 2015, DCA - Nationalt Center for Fødevarer og Jordbrug, Tjele, Denmark.

Børgesen, C.D., Olesen, J.E., 2011. A probabilistic assessment of climate change impacts on yield and nitrogen leaching from winter wheat in Denmark. Natural Hazards and Earth System Sciences, 11(9): 2541-2553. DOI:10.5194/nhess-11-2541-2011

DHI, 2019. User Guide, DHI – Water & Environment, Hørsholm, Denmark.

Diaz, R.J., Rosenberg, R., 2008. Spreading dead zones and consequences for marine ecosystems. Science, 321(5891): 926-9. DOI:10.1126/science.1156401

formaterede: Dansk

formaterede: Dansk

Ernstsen, V., 1996. Reduction of Nitrate By Fe2+ in Clay Minerals. Clays and Clay Minerals, 44(5): 599-608. DOI:10.1346/CCMN.1996.0440503

Ernstsen, V., Mørup, S., 1992. Nitrate reduction in clayey till by Fe(II) in clay minerals. Hyperfine Interactions, 70(1): 1001-1004. DOI:10.1007/BF02397497

Ernstsen, V.H., A.L., Jakobsen, P.R., von Platen,, F., T., L, Hansen, J.R., Blicher-Mathiasen, G.,, Bøgestrand, J., Børgesen, C.D., , 2006. Beregning af nitratreduktionsfaktorer for zonen mellem rodzonen og frem til vandløbet. Data og metode for 1. generationskortet. , Danmarks og Grønlands Geologiske Undersøgelse, Copenhagen, Denmark.

Fleck, S. et al., 2017. Is Biomass Accumulation in Forests an Option to Prevent Climate Change Induced Increases in Nitrate Concentrations in the North German Lowland? , 8(6): 219.

Graham, D.N., Butts, M.B., 2005. Flexible, integrated watershed modelling with MIKE SHE. In: Singh, V.P., Frevert, D.K. (Eds.), Watershed Models, pp. 245-272.

Greve, M.H. et al., 2007. Generating a Danish raster-based topsoil property map combining choropleth maps and point information. Geografisk Tidsskrift, 107.

Hansen, A.L., Christensen, B.S.B., Ernstsen, V., He, X., Refsgaard, J.C., 2014a. A concept for estimating depth of the redox interface for catchment-scale nitrate modelling in a till area in Denmark. Hydrogeology Journal, 22(7): 1639-1655. DOI:10.1007/s10040-014-1152-y

Hansen, A.L., Donnelly, C., Refsgaard, J.C., Karlsson, I.B., 2018. Simulation of nitrate reduction in groundwater - An upscaling approach from small catchments to the Baltic Sea basin. Advances in Water Resources, 111: 58-69. DOI:10.1016/j.advwatres.2017.10.024

Hansen, A.L., Gunderman, D., He, X., Refsgaard, J.C., 2014b. Uncertainty assessment of spatially distributed nitrate reduction potential in groundwater using multiple geological realizations. Journal of Hydrology, 519, Part A: 225-237. DOI:http://dx.doi.org/10.1016/j.jhydrol.2014.07.013

Hansen, A.L., Refsgaard, J.C., Olesen, J.E., Børgesen, C.D., 2017. Potential benefits of a spatially targeted regulation based on detailed N-reduction maps to decrease N-load from agriculture in a small groundwater dominated catchment. Science of The Total Environment, 595: 325-336. DOI:https://doi.org/10.1016/j.scitotenv.2017.03.114

Hansen, B., Dalgaard, T., Thorling, L., S£¿rensen, B., 2012a. Regional analysis of groundwater nitrate concentrations and trends in Denmark in regard to agricultural influence. Biogeosciences Discussions. DOI:10.5194/bgd-9-5321-2012

Hansen, J.R., Ernstsen, V., Refsgaard, J.C., Hansen, S., 2008. Field scale heterogeneity of redox conditions in till-upscaling to a catchment nitrate model. Hydrogeology Journal, 16(7): 1251-1266. DOI:10.1007/s10040-008-0330-1

Hansen, J.R. et al., 2009. An integrated and physically based nitrogen cycle catchment model. Hydrology Research, 40(4): 347-363.

Hansen, S., Abrahamsen, P., T. Petersen, C., Styczen, M., 2012b. Daisy: Model Use, Calibration, and Validation. Transactions of the ASABE, 55(4): 1317. DOI:https://doi.org/10.13031/2013.42244

formaterede: Dansk

formaterede: Dansk

formaterede: Dansk

formaterede: Dansk

Hansen, S., Jensen, H.E., Nielsen, N.E., Svendsen, H., 1991. Simulation of nitrogen dynamics and biomass production in winter wheat using the Danish simulation model DAISY. Fertilizer Research, 27(2-3): 245-259. DOI:10.1007/BF01051131

Hoang, L. et al., 2010. Comparison of the SWAT model versus DAISY-MIKE SHE model for simulating the flow and nitrogen processes. In: conference, T.I.S. (Ed.).

Huno, S.K.M., Rene, E.R., van Hullebusch, E.D., Annachhatre, A.P., 2018. Nitrate removal from groundwater: a review of natural and engineered processes. Journal of Water Supply: Research and Technology-Aqua, 67(8): 885-902. DOI:10.2166/aqua.2018.194

Høgh-Jensen, H., Loges, R., Jørgensen, F.V., Vinther, F.P., Jensen, E.S., 2004. An empirical model for quantification of symbiotic nitrogen fixation in grass-clover mixtures. Agricultural Systems, 82(2): 181-194. DOI:https://doi.org/10.1016/j.agsy.2003.12.003

Højberg, A.L. et al., 2017. Review and assessment of nitrate reduction in groundwater in the Baltic Sea Basin. Journal of Hydrology: Regional Studies, 12: 50-68. DOI:https://doi.org/10.1016/j.ejrh.2017.04.001

Højberg, A.L. et al., 2015a. En ny kvælstofmodel. Oplandsmodel til belastning og virkemidler. Metode rapport (A new nitrogen model. Catchment model for loads and measures. Methodology Report – In Danish). DOI:Available from http://www.geus.dk/DK/water-soil/water-cycle/Documents/national_kvaelstofmodel_metoderapport.pdf

Højberg, A.L. et al., 2010. DK-model2009 – Sammenfatning af opdateringen 2005-2009, Geological Survey of Denmark and Greenland.

Højberg, A.L., Troldborg, L., Stisen, S., Christensen, B.B.S., Henriksen, H.J., 2013. Stakeholder driven update and improvement of a national water resources model. Environmental Modelling & Software, 40(0): 202-213. DOI:http://dx.doi.org/10.1016/j.envsoft.2012.09.010

Højberg, A.L. et al., 2015b. National kvælstofmodel - Oplandsmodel til belastning og virkemidler. Metode rapport, revideret udgave september 2015 (National nitrogenmodel - Catchment model for load and measures. Method report, revised version September 2015). DOI:ISBN 978-87-7871-418-3

Karlsson, I.B. et al., 2014. Significance of hydrological model choice and land use changes when doing climate change impact assessment. In: EGU (Ed.), EGU General Assembly 2014. Geophysical Research Abstracts, Wienna, Austria, pp. 1.

Karlsson, I.B. et al., 2016. Combined effects of climate models, hydrological model structures and land use scenarios on hydrological impacts of climate change. Journal of Hydrology, 535: 301-317. DOI:http://dx.doi.org/10.1016/j.jhydrol.2016.01.069

Karlsson, I.B., Sonnenborg, T.O., Seaby, L.P., Jensen, K.H., Refsgaard, J.C., 2015. The climate change impact of a high-end CO2-emission scenario on hydrology. Climate Research. DOI:doi: 10.3354/cr01265

Knoll, L., Breuer, L., Bach, M., 2020. Nation-wide estimation of groundwater redox conditions and nitrate concentrations through machine learning. Environmental Research Letters, 15(6): 064004. DOI:10.1088/1748-9326/ab7d5c

formaterede: Dansk
formaterede: Dansk
formaterede: Dansk
Feltkode ændret
formaterede: Dansk
formaterede: Dansk
formaterede: Dansk
formaterede: Dansk
formaterede: Dansk
Feltkode ændret
formaterede: Dansk
formaterede: Dansk
formaterede: Dansk

Koch, J., Ernstsen, V., Højberg, A.L., 2019a. Dybden til redoxgrænsen, 100 m grid. In: (GEUS), D.N.G.U.f.D.o.G. (Ed.), Copenhagen, GEUS. DOI:https://data.geus.dk/geusmap/?mapname=denmark#baslay=baseMapDa&optlay=&extent=-139925.69284407864,5929490.944444444,1254925.6928440786,6520509.055555556&layers=redox_dybde_100m_grid

Koch, J. et al., 2019b. Modeling Depth of the Redox Interface at High Resolution at National Scale Using Random Forest and Residual Gaussian Simulation. 55(2): 1451-1469. DOI:10.1029/2018wr023939

Kristensen, K., Jørgensen, U., Grant, R., 2003. Genberegning af modellen N-LES. Baggrundsnotat til Vandmiljøplan II – slutevaluering (Recalculation of the model N-LES. Background note to Aquatic Environmental Plan II – final evaluation). .

Kristensen, K. et al., 2008. Reestimation and further development in the model N-LES - N-LES3 to N-LES4, Aarhus Universitet, Det Jordbrugsvidenskabelige Fakultet.

Kristensen, K.J., Jensen, S.E., 1975. A Model for Estimating Actual Evapotranspiration from Potential Evapotranspiration. Hydrology Research, 6: 170-188.

Kunkel, R., Eisele, M., Schäfer, W., Tetzlaff, B., Wendland, F., 2008. Planning and implementation of nitrogen reduction measures in catchment areas based on a determination and ranking of target areas. Desalination, 226(1): 1-12. DOI:https://doi.org/10.1016/j.desal.2007.01.231

Madsen, H., 2000. Automatic calibration of a conceptual rainfall-runoff model using multiple objectives. Journal of Hydrology, 235: 276-288. DOI:10.1016/S0022-1694(00)00279-1

Mas-Pla, J., Menció, A., 2019. Groundwater nitrate pollution and climate change: learnings from a water balance-based analysis of several aquifers in a western Mediterranean region (Catalonia). Environ Sci Pollut Res Int, 26(3): 2184-2202. DOI:10.1007/s11356-018-1859-8

Merz, C., Steidl, J., Dannowski, R., 2009. Parameterization and regionalization of redox based denitrification for GIS-embedded nitrate transport modeling in Pleistocene aquifer systems. Environ Geol, 58(7): 1587-1599. DOI:10.1007/s00254-008-1665-6

Møller, J. et al., 2005. Fodermiddeltabel - Sammensætning og foderværdi af fodermidler til kvæg. 64.

Nielsen, K. et al., 2000. Areal Informations Systemet - AIS. , National Environmental Research Institute, Denmark.

Olesen, J.E. et al., 2019. Nitrate leaching losses from two Baltic Sea catchments under scenarios of changes in land use, land management and climate. Ambio, 48(11): 1252-1263. DOI:10.1007/s13280-019-01254-2

Olesen, J.E. et al., 2014. Scenarier for fremtidens arealanvendelse i Danmark. Vand og Jord, 21(3): 126-129.

Ortmeyer, F., Mas-Pla, J., Wohnlich, S., Banning, A., 2021. Forecasting nitrate evolution in an alluvial aquifer under distinct environmental and climate change scenarios (Lower Rhine Embayment, Germany). Science of The Total Environment, 768: 144463. DOI:https://doi.org/10.1016/j.scitotenv.2020.144463

Paradis, D. et al., 2016. Groundwater nitrate concentration evolution under climate change and agricultural adaptation scenarios: Prince Edward Island, Canada. Earth Syst. Dynam., 7(1): 183-202. DOI:10.5194/esd-7-183-2016

formaterede: Dansk

formaterede: Dansk

formaterede: Dansk

formaterede: Dansk

formaterede: Dansk

Postma, D., Boesen, C., Kristiansen, H., Larsen, F., 1991. Nitrate Reduction in an Unconfined Sandy Aquifer: Water Chemistry, Reduction Processes, and Geochemical Modeling. Water Resources Research, 27(8): 2027-2045. DOI:10.1029/91wr00989

Quick, A.M. et al., 2019. Nitrous oxide from streams and rivers: A review of primary biogeochemical pathways and environmental variables. Earth-Science Reviews, 191: 224-262. DOI:https://doi.org/10.1016/j.earscirev.2019.02.021

Refsgaard, J.C. et al., 2019. Spatially differentiated regulation: Can it save the Baltic Sea from excessive N-loads? Ambio, 48(11): 1278-1289. DOI:10.1007/s13280-019-01195-w

Refsgaard, J.C. et al., 2011. Vandbalance i Danmark - Vejledning i opgørelse af vandbalance ud fra hydrologiske data for perioden 1990-2010, Copenhagen, Denmark.

Reusch, T.B.H. et al., 2018. The Baltic Sea as a time machine for the future coastal ocean. Science Advances, 4(5): eaar8195. DOI:10.1126/sciadv.aar8195

Seaby, L.P. et al., 2013. Assessment of robustness and significance of climate change signals for an ensemble of distribution-based scaled climate projections. Journal of Hydrology, 486: 479–493.

Sjøeng, A.M.S., Kaste, Ø., Wright, R.F., 2009. Modelling future NO3 leaching from an upland headwater catchment in SW Norway using the MAGIC model: II. Simulation of future nitrate leaching given scenarios of climate change and nitrogen deposition. Hydrology Research, 40(2-3): 217-233. DOI:10.2166/nh.2009.068

Statistikbanken, 2015. Statistical regional registrated annual mean yields. (In Danish) https://www.statistikbanken.dk/jord3

Styczen, M. et al., 2004. Standardopstillinger til Daisy-modellen. Vejledning og baggrund, Institut for Vand og Miljø, DHI.

Tesoriero, A.J., Terziotti, S., Abrams, D.B., 2015. Predicting Redox Conditions in Groundwater at a Regional Scale. Environmental Science & Technology, 49(16): 9657-9664. DOI:10.1021/acs.est.5b01869

Troldborg, L. et al., 2010. DK-model2009 - Modelopstilling og kalibrering for Fyn. .

Trolle, D. et al., 2019. Effects of changes in land use and climate on aquatic ecosystems: Coupling of models and decomposition of uncertainties. Science of The Total Environment, 657: 627-633. DOI:https://doi.org/10.1016/j.scitotenv.2018.12.055

van Genuchten, M.T., 1980. A Closed-form Equation for Predicting the Hydraulic Conductivity of Unsaturated Soils. 44(5): 892-898. DOI:10.2136/sssaj1980.03615995004400050002x

van Vuuren, D.P. et al., 2011. The representative concentration pathways: an overview. Climatic Change, 109(1): 5. DOI:10.1007/s10584-011-0148-z

Windolf, J. et al., 2016. Successful reduction of diffuse nitrogen emissions at catchment scale: example from the pilot River Odense, Denmark. Water science and technology : a journal of the International Association on Water Pollution Research, 73(11): 2583-9. DOI:10.2166/wst.2016.067

Wriedt, G., Rode, M., 2006. Modelling nitrate transport and turnover in a lowland catchment system. Journal of Hydrology, 328(1): 157-176. DOI:https://doi.org/10.1016/j.jhydrol.2005.12.017

formaterede: Dansk

formaterede: Dansk

formaterede: Dansk

formaterede: Dansk

Feltkode ændret

formaterede: Dansk

Wulff, F. et al., 2014. Reduction of Baltic Sea Nutrient Inputs and Allocation of Abatement Costs Within the Baltic Sea Catchment. AMBIO, 43(1): 11-25. DOI:10.1007/s13280-013-0484-5

Side 23: [1] Formateret **Ida Karlsson** **09-04-2021 10:06:00**

Venstre, Linjeafstand: enkelt

Side 23: [2] formaterede **Ida Karlsson** **08-04-2021 12:13:00**

Engelsk (USA)

Side 23: [3] formaterede **Ida Karlsson** **08-04-2021 12:13:00**

Engelsk (USA)

Side 23: [4] formaterede **Ida Karlsson** **08-04-2021 12:13:00**

Engelsk (USA)

Side 23: [5] formaterede **Ida Karlsson** **08-04-2021 12:13:00**

Engelsk (USA)

Side 23: [6] formaterede **Ida Karlsson** **08-04-2021 12:13:00**

Engelsk (USA)

Side 23: [7] formaterede **Ida Karlsson** **08-04-2021 12:13:00**

Engelsk (USA)

Side 23: [8] formaterede **Ida Karlsson** **08-04-2021 12:13:00**

Engelsk (USA)

Side 23: [9] formaterede **Ida Karlsson** **08-04-2021 12:13:00**

Engelsk (USA)

Side 23: [10] formaterede **Ida Karlsson** **08-04-2021 12:13:00**

Engelsk (USA)

Side 23: [11] formaterede **Ida Karlsson** **08-04-2021 12:13:00**

Engelsk (USA)

Side 23: [12] formaterede **Ida Karlsson** **08-04-2021 12:13:00**

Engelsk (USA)

Side 23: [13] formaterede **Ida Karlsson** **08-04-2021 12:13:00**

Engelsk (USA)

Side 23: [14] formaterede **Ida Karlsson** **08-04-2021 12:13:00**

Engelsk (USA)

Side 23: [15] formaterede **Ida Karlsson** **08-04-2021 12:13:00**

Engelsk (USA)

Side 23: [16] formaterede **Ida Karlsson** **08-04-2021 12:13:00**

Engelsk (USA)

Side 23: [17] formaterede **Ida Karlsson** **08-04-2021 12:13:00**

Engelsk (USA)

Side 23: [18] formaterede **Ida Karlsson** **08-04-2021 12:13:00**

Engelsk (USA)

Side 23: [19] formaterede **Ida Karlsson** **08-04-2021 12:13:00**

Engelsk (USA)

Side 23: [20] formaterede **Ida Karlsson** **08-04-2021 12:13:00**

Engelsk (USA)

Side 23: [21] formaterede **Ida Karlsson** **08-04-2021 12:13:00**

Engelsk (USA)

Side 23: [22] formaterede **Ida Karlsson** **08-04-2021 12:13:00**

Engelsk (USA)

Side 23: [23] formaterede **Ida Karlsson** **08-04-2021 12:13:00**

Engelsk (USA)

Side 23: [24] formaterede **Ida Karlsson** **08-04-2021 12:13:00**

Engelsk (USA)

Side 23: [25] formaterede **Ida Karlsson** **08-04-2021 12:13:00**

Engelsk (USA)

Side 23: [26] formaterede **Ida Karlsson** **08-04-2021 12:13:00**

Engelsk (USA)

Side 23: [27] formaterede **Ida Karlsson** **08-04-2021 12:13:00**

Engelsk (USA)

Side 23: [28] formaterede **Ida Karlsson** **08-04-2021 12:13:00**

Engelsk (USA)

Side 23: [29] formaterede **Ida Karlsson** **08-04-2021 12:13:00**

Engelsk (USA)

Side 23: [30] formaterede **Ida Karlsson** **08-04-2021 12:13:00**

Engelsk (USA)

Side 23: [31] formaterede **Ida Karlsson** **08-04-2021 12:13:00**

Engelsk (USA)

Side 23: [32] formaterede **Ida Karlsson** **08-04-2021 12:13:00**

Engelsk (USA)

Side 23: [33] formaterede **Ida Karlsson** **08-04-2021 12:13:00**

Engelsk (USA)

Side 23: [34] formaterede **Ida Karlsson** **08-04-2021 12:13:00**

Engelsk (USA)

Side 23: [35] formaterede **Ida Karlsson** **08-04-2021 12:13:00**

Engelsk (USA)

Side 23: [36] formaterede **Ida Karlsson** **08-04-2021 12:13:00**

Engelsk (USA)

Side 23: [37] formaterede **Ida Karlsson** **08-04-2021 12:13:00**

Engelsk (USA)

Side 23: [38] formaterede **Ida Karlsson** **08-04-2021 12:13:00**

Engelsk (USA)

Side 23: [39] formaterede **Ida Karlsson** **08-04-2021 12:13:00**

Engelsk (USA)

Side 23: [40] formaterede **Ida Karlsson** **08-04-2021 12:13:00**

Engelsk (USA)

Side 23: [41] formaterede **Ida Karlsson** **08-04-2021 12:13:00**

Engelsk (USA)

Side 23: [42] formaterede **Ida Karlsson** **08-04-2021 12:13:00**

Engelsk (USA)

Side 23: [43] formaterede **Ida Karlsson** **08-04-2021 12:13:00**

Engelsk (USA)

Side 23: [44] formaterede **Ida Karlsson** **08-04-2021 12:13:00**

Engelsk (USA)

Side 23: [45] formaterede **Ida Karlsson** **08-04-2021 12:13:00**

Engelsk (USA)

Side 23: [46] formaterede **Ida Karlsson** **08-04-2021 12:13:00**

Engelsk (USA)

Side 23: [47] formaterede **Ida Karlsson** **08-04-2021 12:13:00**

Engelsk (USA)

Side 23: [48] formaterede **Ida Karlsson** **08-04-2021 12:13:00**

Engelsk (USA)

Side 23: [49] formaterede **Ida Karlsson** **08-04-2021 12:13:00**

Engelsk (USA)

Side 23: [50] formaterede **Ida Karlsson** **08-04-2021 12:13:00**

Engelsk (USA)